

**The role of the ribosomal protein S19 C-terminus in Gi protein-dependent alternative activation of p38 MAP kinase *via* the C5a receptor in HMC-1 cells**

**Hiroshi Nishiura<sup>1</sup> · Kazutaka Tokita<sup>1</sup> · Ying Li<sup>1</sup> · Koichi Harada<sup>2</sup> · Trent M. Woodruff<sup>3</sup> · Stephean M. Taylor<sup>3</sup> · Tienabe K. Nsiama<sup>4</sup> · Norikazu Nishino<sup>4</sup> · Tetsuro Yamamoto<sup>1</sup>**

<sup>1</sup>Department of Molecular Pathology, Faculty of Life Sciences, Kumamoto University Graduate School, Kumamoto, Japan.

<sup>2</sup>Department of health preservation, Faculty of Medicine, Kumamoto University, Kumamoto, Japan.

<sup>3</sup>School of Biomedical Sciences, University of Queensland, Brisbane, Australia.

<sup>4</sup>Department of Biological Functions and Engineering, Graduate School of Life Science and Systems Engineering, Kyushu Institute of Technology, Kitakyushu, Japan.

**Corresponding author:** Hiroshi Nishiura. E-mail address: [seino@kumamoto-u.ac.jp](mailto:seino@kumamoto-u.ac.jp) Telephone number; 81963735306. Fax number; 81963735308.

**A list of key words:** C5a receptor, Gi protein, HMC-1 cells, p38MAPK, PI3K, ribosomal protein S19.

## Materials and methods

### Animals

Specific Pathogen Free Albino-Hartley strain male guinea pigs (400-550 g body weight) were purchased from Kyudo Corp. (Kumamoto, Japan). They were kept in the Center for Animal Resources and Development of Kumamoto University. The animal experiments were performed under regulations established by the Ethical Committee for Animal Experiments of Kumamoto University School of Medicine.

### Measurement of plasma extravasation

Plasma extravasation was measured using the dye-extraction method. In brief, at 15 min after the intravenous injection of Evans blue dye solution (2.5% in 0.6% saline), each sample (0.1 ml) was intradermally injected into two guinea pigs at three different experiments. At 30 min after the injection, the guinea pigs were killed by exsanguination under ether anesthesia, and 14-mm diameter skin lesions were punched out. The extravasated Evans blue dye in each lesion was extracted in 3 ml formamide for 72 h at 60°C, and the absorbance of the extract was measured at 620 nm using a spectrophotometer (U-2000A, Hitachi). Each measured value was converted into the amount of extravasated dye ( $\mu\text{g}/\text{site}$ ). In inhibition experiments, the amount of dye was further converted to a relative permeability to  $10^{-7}$  M C5a-induced one (100%).

### Separation of resident mast cells from guinea pig abdomens

Resident cells ( $2 \times 10^7$  cells/body) were recovered from guinea pig abdomens in 40 ml of PBS. After centrifugation at 1,200 rpm for 5 min at room temperature, resident cells were re-suspended in 1 ml of Dulbecco's Modified Eagle Medium containing 10% fetal bovine serum (Gibco BRC, Paisley, Scotland) and put on 4 ml of Ficoll paque gradient. After centrifugation at 1,200 rpm for 20 min at 4°C, about 2% resident mast cells ( $4 \times 10^5$  cells/body) were separated into the 80% layer and were adjusted to  $5 \times 10^5$  cells/ml for chemotaxis chamber assay. The purity of mast cells in the 80% layer was over 98% in the pathological finding with Giemsa solution.

### Separation of CD14<sup>+</sup> cells from human venous blood

Monocytes and neutrophils were isolated from heparinized human venous blood of at least three different healthy donors. CD14<sup>+</sup> cells were separated as monocytes/macrophages from monocytes by using MACS column (Miltenyi Biotec K.K., Tokyo, Japan) according to an instruction manual. In brief, after washing cells in the monocyte layer of Ficoll-Paque™ PLUS (GE healthcare, Uppsala, Sweden) two times in 10 ml of a cold Ca<sup>2+</sup> buffer [Hanks' balanced salt solution containing 20 mM HEPES and 3% BSA, pH. 7.4],  $1 \times 10^8$  monocytes were resuspended in 500  $\mu\text{l}$  of the same cold Ca<sup>2+</sup> buffer containing 80  $\mu\text{l}$  of CD14 micro-beads. 15 min later, 500 $\mu\text{l}$  of monocytes were applied to MACS LS column on magnetic MACS MULTI-STAND. After washing three times in 3 ml of the cold Ca<sup>2+</sup> buffer, MACS LS column was separated and CD14<sup>+</sup> cells were eluted in 5 ml of Dulbecco's Modified Eagle Medium containing 10% fetal bovine serum. We usually got about 20% positive cells from monocytes. The purity of CD14<sup>+</sup> cells and neutrophils were observed over 98% by fluorescence-activated cell sorting.

## Abstract

We have demonstrated that an alternative C5a receptor (C5aR) ligand, the homodimer of ribosomal protein S19 (RP S19), contains a unique C-terminus (I<sub>134</sub>-H<sub>145</sub>) that is distinct from the moieties involved in the C5a-C5aR interaction. To examine the role of I<sub>134</sub>-H<sub>145</sub> in the ligand-C5aR interaction, we connected this peptide to the C-terminus of C5a (C5a/RP S19) and found that it endowed the second binding moiety of RP S19 (L<sub>131</sub>DR) with a relatively higher binding affinity to the C5aR on a human mast cell line, HMC-1. In contrast to the C5aR, the second C5aR C5L2 worked as a decoy receptor. As a result, the mitogen-activated protein kinase (MAPK) downstream of the Gi protein exchanged extracellular-signal regulated kinase for p38MAPK. This alternative p38MAPK activation could be pharmacologically suppressed not only by the downregulation of phosphoinositide 3-kinase (PI3K) by LY294002, but also by the over-activation of protein kinase C by phorbol 12-myristate 13-acetate. The activation was reproduced upon C5a-C5aR interaction by a simultaneous suppression of PI3K and phospholipase C with LY294002 and U73122 at low concentrations. Moreover, p38MAPK phosphorylation upstream of the pertussis toxin-dependent extracellular Ca<sup>2+</sup> entry was also suppressed by high concentrations of MgCl<sub>2</sub>, which blocks melastatin-type transient receptor potential Ca<sup>2+</sup> channels (TRPMs). The active conformation of C5aR upon the ligation by C5a, at least on HMC-1 cells, is changed by the additional interaction of the I<sub>134</sub>-H<sub>145</sub> peptide, which seems to guide the alternative activation of p38MAPK. This activation is then amplified by a novel positive feedback loop between p38MAPK and TRPM.

## Introduction

The structure of the C5a receptor (C5aR) gene is well-characterized and known not to generate any alternative splice variants [1]. The active form of C5aR catalyzes the activation of the trimeric Gai2βy protein that in turn, activates phosphoinositide 3-kinase (PI3K), which directly activates the leukocyte chemotaxis and secretion [2, 3]. The active conformation of C5aR is changed by the complementary C5a-derived anaphylatoxin C5a, which classically has been considered to be the universal C5aR agonist. The interaction between C5a and C5aR is accomplished by a two-step binding sequence: the basic cluster of C5a initially attaches to the extracellular NH<sub>2</sub>-terminal acidic domain of C5aR, and then the C-terminus of C5a (L<sub>72</sub>GR<sub>74</sub>) interacts with the second binding site of C5aR within the transmembrane core [4]. The second binding event simultaneously amplifies the canonical phospholipase Cβ2 (PLCβ2)-PI3K pathway through the positive feedback loop between the inositol 1,4,5-trisphosphate receptor (IP3R) and the Ca<sup>2+</sup> release-activated Ca<sup>2+</sup> channel (CRAC). This positive feedback loop for the mobilization of intracellular/extracellular Ca<sup>2+</sup> contributes to the full leukocyte response [2].

We have demonstrated that the ribosomal protein S19 (RP S19) homodimer is an alternative ligand for C5aR [5-7]. The RP S19 dimer has an intermolecular cross-linkage between Lys122 and Gln137 that is formed by a transglutaminase-catalyzed reaction in cells undergoing apoptosis [8-11]. Although there is no shared ancestry between RP S19 and C5a, we found similar first and second binding moieties in RP S19 and C5a [7, 12]. The first receptor-binding moiety is a basic cluster (K<sub>38</sub>LAKHK<sub>43</sub>). The second is L<sub>131</sub>DR<sub>133</sub>, where the β-carboxyl residue of Asp132 in RP S19 is functionally equivalent to the α-carboxyl residue of the C-terminal Arg74 in C5a [12, 13]. Therefore, we hypothesized that the C5aR on phagocytic leukocytes bound by the RP S19 dimer would select the same intracellular signal transduction pathway as the common pathway involved in the C5a-C5aR interaction. However, the alternative ligand elicits different effects on chemotaxis and secretion in a cell-type specific manner; i.e., it behaves as a C5aR agonist and antagonist on monocytes and neutrophils, respectively [14, 15]. A unique moiety is present at the C-terminus of RP S19 (I<sub>134</sub>-H<sub>145</sub>). When I<sub>134</sub>-H<sub>145</sub> was deleted from the RP S19 dimer, the dimer lost its antagonist-induced effect on neutrophil chemotaxis [13]. These data suggested that there might be a modulator near the C5aR on neutrophils that interacts with I<sub>134</sub>-H<sub>145</sub> to turn off the common switch.

To examine the role of I<sub>134</sub>-H<sub>145</sub> in C5aR function, we prepared several tools to substitute for the RP S19 dimer (unpublished data of Nishiura *et al.*). We recently prepared a recombinant C5a chimera protein (C5a/RP S19) with I<sub>134</sub>-H<sub>145</sub> connected to the C-terminus of C5a. The guinea pig is relatively well-recognized as a useful experimental model for studies of the behavior of human C5a *in vivo* [16]. We also have demonstrated that this animal is the best experimental model to examine the role of the RP S19 dimer *in vivo* [17]. The amino acid sequence of guinea pig RP S19 is identical to that of the human. Therefore, C5a/RP S19 protein, containing the human amino acid sequence, results in monocyte-predominant infiltration when injected intradermally. This response occurs even when human C5a and the RP S19 dimer are present simultaneously [15, 18]. From these *in vivo* results, we propose that the combined use of C5a and C5a/RP S19 will allow the analysis of the role of I<sub>134</sub>-H<sub>145</sub> in C5aR function for any cell-type or cell-state.

C5aR gene expression has been demonstrated in various non-myeloid cells, including microvascular endothelial cells, articular chondrocytes, and stimulated hepatocytes [2]. However, the role of C5aR in non-myeloid cells is largely unknown. We have reported the *de novo* synthesis of C5aR in apoptosis-initiated mouse NIH3T3 cells that do not constantly express the C5aR gene [19]. In this case, both the RP S19 dimer and C5a behaved as C5aR agonists. However, they produced opposite outcomes; while the RP S19 dimer-C5aR interaction accelerated apoptosis in an autocrine/paracrine fashion, the C5a-C5aR interaction bypassed apoptosis when C5a was present. We recently confirmed this result in human cancer cell lines using C5a and C5a/RP S19 in combination and observed the suppression of extracellular-signal regulated kinase (ERK) phosphorylation [20]. Moreover, we did not observe any difference in binding affinities between C5a and the RP S19 dimer to the C5aR on neutrophils [8]. However, when using synthetic peptides that mimic the second binding moieties of C5a, with or without the RP S19 C-terminus, we found that the C5a/RP S19 peptide (YSFKDMLDRIAGQVAAANKKH) had a relatively higher binding affinity for the C5aR on neutrophils at high concentrations than did the C5a peptide (YSFKDMLGR).

These data and published literature lead us to hypothesize that the relatively greater binding affinity of the RP S19 dimer to the C5aR (on any cell type), stimulated by an additional interaction of I<sub>134</sub>-H<sub>145</sub>, would

activate an alternative intracellular signal transduction pathway distinct from the trimeric Gai2 $\beta$ γ protein-dependent amplification of the canonical PLC $\beta$ 2-PI3K pathway (i.e., the positive feedback loop between IP3R and CRAC) [2, 3]. We hypothesized that a trimeric Gai2 $\beta$ γ protein-dependent amplification of an alternative PI3K pathway creates a novel positive feedback loop. To test this hypothesis, we first examined whether the C5aR agonist-induced effects of C5a/RP S19 on histamine release and chemotaxis were reproduced in guinea pig cutaneous and abdomen mast cells, respectively (Supplemental Fig. 1-2). We then examined the alternate pathway in a long-term human mast cell line, HMC-1 [21].

## Materials and methods

### Chemicals and antibodies

Dulbecco's Modified Eagle Medium (DMEM), Minimum Essential Medium (MEM), and fetal bovine serum (FBS) were products of Gibco BRC (Paisley, Scotland). Hanks' balanced salt solution (HBSS) was a product of Nissui Pharmaceutical Co. (Tokyo, Japan). Fura2-AM and HEPES buffer were products of Dojindo Laboratories (Kumamoto, Japan). ECL Plus Western Blotting Detection System was obtained from Amersham Biosciences KK (Tokyo, Japan). Bovine serum albumin (BSA),  $\alpha$ -thioglycerol, human fibronectin, phorbol-12 myristate 13-acetate (PMA) formyl-Met-Leu-Phe (fMLP), pertussis toxin (PTX, catalyst of the ADP-ribosylation of Gai and Gao proteins), inhibitors against PLC (U73122), PI3K (LY294002), ERK (PD98059), p38 mitogen-activated protein kinase (p38MAPK) (SB203580), phospholipase A<sub>2</sub> (PLA<sub>2</sub>) as well as PLA<sub>2</sub>-dependent transient receptor potential channel (TRP) [ACA; N-(*p*-amylcinnamoyl)anthranilic acid] [22], another TRP (Ruthenium Red), and CRAC (2-APB; 2-aminorthyl dephenylborinate) were purchased from Sigma Chemical (ST. Louis, MI). A multiwell chamber for chemotaxis assay was a product of Neuro Probe (Bethesda, MD). Nucleopore filters were purchased from Nucleopore (Pleasant, CA). Immobilor Transfer Membrane™ was a product of Millipore (Billerica, MA). Anti-C5aR, anti-Akt, anti-phosphorylated (p)-Akt, anti-ERK, anti-p-ERK rabbit IgGs, phycoerythrin (PE)-conjugated anti-C5aR mouse IgG, and anti-C5aR, anti-C5L2, horseradish peroxidase (HRP)-conjugated anti-rabbit IgG goat IgGs were products of Santa Cruz Biotechnology (Santa Cruz, CA). Anti-stress-activated protein kinase/c-Jun N-terminus kinase (JNK), anti-p-JNK, anti-p38MAPK, and anti-p-p38MAPK rabbit IgGs were products of Cell Signaling Technology® (Boston, USA). Block Ace™ was purchased from Dainippon Pharmaceutical (Suita, Japan). All other chemicals were obtained from Nacalai Tesque (Kyoto, Japan) or from Wako Pure Chemicals (Osaka, Japan) unless otherwise specified.

N-[(4-Dimethylaminophenyl)methyl]-N-(4-isopropylphenyl)-7-methoxy-1,2,3,4-tetrahydronaphthalen-1-carboxamide, HCl [23] and N<sup>2</sup>-[(2,2-Diphenylethoxy)acetyl]-L-arginine, TFA [24] were purchased as a C5aR antagonist (W-54011) and a C3aR antagonist/partial agonist (SB-290157) from Merck KGaA (Darmstadt, FRG), respectively. NMePhe-Lys-Pro-dCha-dCha-dArg [25] and Ac-Phe-[Orn-Pro-dCha-Trp-Arg] [26] were respectively prepared as a C5aR antagonistic/partial agonistic peptide (C5aRA) and a C5aR antagonist (PMX-53). The antagonistic effects of C5aRA at 10<sup>-6</sup> M and of PMX-53 at 10<sup>-7</sup> M were confirmed in a C5a-induced leukocyte chemotaxis assay (data not shown). The recombinant C5a and C5a/RP S19 were prepared as described previously [18]. These proteins possessed the S-tag at the N-terminus. In the recombinant C5a and C5a/RP S19, Cys27 was substituted by Arg, and Gly73 of C5a/RP S19 was substituted by Asp. These recombinant proteins demonstrated single bands in polyacrylamide gel electrophoresis in the presence of sodium dodecyl sulfate (SDS-PAGE) and in western blotting (data not shown).

### Cell line

HMC-1 cells were kindly gifted by Dr. Joseph H. Butterfield of Mayo Clinic, USA.

### Binding competition assay with radio-labeled C5aR ligands

Aliquots of the YSFKDMQLGR peptide and the recombinant C5a and C5a/RP S19 were radio-labeled with <sup>125</sup>I using Iodobeads (Pierce, Rockford, USA) according to the manufacturer's instruction manual. In binding competition assays to estimate the receptor binding affinity, one of the radio-labeled peptide fragment and recombinant proteins was mixed with HMC-1 cells (2 × 10<sup>6</sup> cells/ml) in HBSS containing 20 mM HEPES and 0.5% BSA (pH 7.4) at a putative final concentration of 10<sup>-7</sup> M and 10<sup>-8</sup> M, respectively, in the absence or presence of various concentrations of unlabeled C5aR ligands [14]. In binding inhibition assays to identify

the receptor, HMC-1 cells were pretreated with either 2 µg/ml anti-C5aR rabbit IgG, 2 µg/ml control rabbit IgG, 2 µg/ml anti-C5L2 goat IgG, 2 µg/ml control goat IgG, one of 10<sup>-7</sup> M C5aR antagonists (PMX-53 and W54011), or 2 × 10<sup>-7</sup> M C3aR antagonist/partial agonist peptide (SB-290157) at 4°C for 30 min, and the cells were then mixed with either of the <sup>125</sup>I-recombinant proteins (C5a and C5a/RP S19). The mixtures of HMC-1 cells and a radio-labeled ligand were then incubated on ice for 60 min, and unbound radio-labeled molecules were separated from the cells by centrifugation at 500 × g for 2 min at 4°C. After washing the cells 3 times in the fresh medium, radioactivity on the cells was measured for 2 min in a gamma counter (PerkinElmer, Yokohama, Japan).

#### Fluorescence-activated cell sorting (FACS) analyses

For analysis of C5aR internalization, HMC-1 cells (2 × 10<sup>6</sup> cells/ml) in HBSS containing 20 mM HEPES and 0.5% BSA (pH 7.4) were stimulated with 10<sup>-8</sup> M C5a, 10<sup>-7</sup> M C5a/RP S19, and the mixture at 37°C for 10 min and 30 min, respectively. After washing in 1 ml of cold phosphate-buffered saline (PBS) containing 5% FBS (FACS medium) at 3 times, cells were incubated with PE-conjugated anti-C5aR monoclonal antibody for 30 min at 4°C. The mean intensity of PE on cells was analyzed as the number of cell surface expressing C5aR using a FACS Caliber flow cytometer (BD, Tokyo, Japan).

#### Calcium imaging

HMC-1 cells (2 × 10<sup>6</sup> cells/ml) were loaded with the calcium-sensitive Fura 2-AM (1 µM) in the Ca<sup>2+</sup> buffer (HBSS containing 20 mM HEPES and 3% BSA, pH. 7.4) for 30 min at 37°C according to the instruction manual (Dojindo Laboratories). After washing with the Ca<sup>2+</sup> buffer or the Ca<sup>2+</sup> free buffer (MEM medium containing 20 mM HEPES, 3% BSA, and 2 mM EGTA, pH. 7.4), the cells were respectively re-suspended in the same buffer used for the cell washing. Samples were placed directly into the cell suspension in cuvette after a 5-min baseline recording. Recordings were made with an F-2500 calcium imaging system with FL Solutions (Hitachi, Tokyo, Japan) that calculated the ratio of fluorescent signals obtained at 37°C with excitation wavelengths at 340 and at 380 nm and with an emission wavelength at 510 nm. In some inhibition experiments, the recording charts are expressed as percent fluorescent activity to the maximum observed without the inhibitor.

#### Western blotting analysis

Electrophoresis was performed on a vertical slab gel of 12% polyacrylamide according to the method of Laemmli [27]. Transference of proteins from the SDS-PAGE to a membrane was performed electrophoretically according to the method of Kyhse-Anderson with some modifications using a Semi Dry Electroblotter (Sartorius) for 90 min with an electric current of 15 V [28]. The membrane was treated with Block Ace<sup>™</sup> (4%) for 30 min at 22°C. The first reaction was performed with one of rabbit IgG against whole protein or against phosphorylated protein of Akt, ERK, p38MAPK, or JNK at 100 ng/ml in PBS containing 0.03% Tween 20 for 1 h at 22°C. After washing in the same buffer, the sec reaction was performed with HRP-conjugated anti-rabbit IgG goat IgG (20 ng/ml) for 30 min at 22°C. After washing, the enhanced chemiluminescence (ECL) reaction was performed on the membrane with ECL Plus Western Blotting Detection System<sup>™</sup>. The ratio of phosphorylated protein was determined using NIH Image 1.63 image analysis software; relative rate of the phosphorylated protein to the total protein = (density of phosphorylated band / density of total band) × 100%.

#### Histamine release assay

HMC-1 cells (2 × 10<sup>6</sup> cells/ml) in a mast cell medium (150 mM NaCl, 3.7 mM KCl, 3 mM Na<sub>2</sub>HPO<sub>4</sub>, 3.5 mM KH<sub>2</sub>PO<sub>4</sub>, 5.6 mM glucose, 0.1% gelatin, 0.1% BSA, and 1 mM CaCl<sub>2</sub>, pH 6.8) were stimulated with 10<sup>-8</sup> M C5a for 10 min at 37°C in the absence or presence of various concentrations of C5a/RP S19 according to Shore's method [29]. After centrifugation at 10,000 g for 1 min at 22°C, the supernatant was separated and the precipitated cells were lysed in the mast cell medium but containing 1 % Triton X-100 (1 ml) for 15 min at 4°C. Histamine concentrations in the supernatant and in the cell lysate were measured as the fluorescent signal using an F-2500 quantification system with FL Solutions (Hitachi, Tokyo, Japan) that calculated the fluorescent signal to the histamine concentration at 22°C with excitation and emission wavelengths at 360 nm and at 450 nm, respectively. Results are shown as the percent ratio of released histamine in the

supernatant to the total cellular histamine content; = concentration of histamine in the supernatant / (concentration of histamine in the supernatant and in the cells) X 100. Some results were also converted into percent activity to the maximum.

### Chemotaxis assay

HMC-1 cells ( $2 \times 10^6$  cells/ml) in DMEM medium containing 10% FBS were prepared for the multiwell chamber assay. The multiwell chamber assay was performed according to the method of Falk et al. using a Nucleopore filter with a pore size of 8  $\mu\text{m}$  [21, 30, 31]. Before the chemotaxis assay, the upper wells of 48-well chemotaxis chamber were coated with 10  $\mu\text{g/ml}$  human fibronectin for 30 min. After incubation for 180 min, the membrane was separated, fixed with methanol, and stained with Giemsa solution. The total number of cells that migrated beyond the lower surface of the membrane was counted in five microscopic high-power fields. The results are expressed as the number of migrated cells. Sometimes results were converted into percent activity to the maximum.

### Effects of signal pathway inhibitors

When the effects of signal pathway inhibitors on the cellular responses were examined with 100 ng/ml PTX, 2  $\mu\text{M}$  U73122, 2  $\mu\text{M}$  LY294002, 50  $\mu\text{M}$  PD98059, 10  $\mu\text{M}$  SB203580, 10  $\mu\text{M}$  ACA, 10  $\mu\text{M}$  Ruthenium Red, 50  $\mu\text{M}$  2-APB or their negative control PBS, HMC-1 cells ( $2 \times 10^6$  cells/ml) were pretreated for 60 min at 37°C and were stimulated with  $10^{-8}$  M C5a,  $10^{-7}$  M C5a/RP S19 and  $10^{-8}$  M RP S19 dimer, respectively.

### Statistical analysis

The results of representative examinations were confirmed by multiple experiments with triplicate samples. Statistical significance was calculated by the non-parametric or parametric tests offered in the two way analysis of variance (ANOVA) window, respectively. Values are expressed as mean  $\pm$  SD. A p-value  $<0.05$  was considered statistically significant and shown as  $P<0.05$ : \* and  $P<0.01$ : \*\*.

## Results

### C5aR agonist-induced histamine release and chemotaxis of HMC-1 cells

To examine the agonist-induced effects of C5a/RP S19 as a substitute for the RP S19 dimer on the C5aR of guinea pig cutaneous mast cells, various concentrations of C5a/RP S19, C5a, or mixtures of both were injected intradermally. Evans blue dye was used to measure vascular permeability enhancement (VPE) for 30 min (Supplemental Fig. 1) [32]. C5a/RP S19 exhibited the C5aR agonist-induced VPE at relatively high concentrations in comparison with C5a. The difference between C5a/RP S19 and C5a was also detected in chemotaxis assays with resident guinea pig abdomen mast cells (Supplemental Fig. 2). These data indicated that the C5aR agonist-induced effects of C5a/RP S19 on histamine release and chemotaxis could be reproduced in human mast cells.

To examine the specific role of the C-terminus of RP S19 ( $\text{I}_{134}\text{-H}_{145}$ ), we confirmed the agonist-induced effects of both C5a/RP S19 and C5a in HMC-1 cells, which constantly express C5aR. As shown in Fig. 1A, C5a induced histamine release in a dose-dependent manner at concentrations ranging from  $10^{-9}$  M to  $10^{-7}$  M. C5a/RP S19 also induced a significant histamine release at relatively higher concentrations than C5a. As in the case of C5a-induced reaction, the C5a/RP S19-induced histamine release was modified neither by a blockade of C3aR, SB-290157, nor by that of C5L2, anti-C5L2 goat IgG, whereas it was suppressed by any one of C5aR blockades such as C5aRA, PMX-53, W-54011, and anti-C5aR rabbit IgG (Fig. 1B).

The apparent C5aR antagonist-induced effects of C5a/RP S19 at lower concentrations, such as  $10^{-9}$  M and  $10^{-8}$  M, was obvious; the activity induced by  $10^{-8}$  M C5a was reduced to about 75% and 33%, respectively (Fig. 1C). This indicates that  $10^{-9}$  M and  $10^{-8}$  M C5a/RP S19 have competitive potencies of 25% and 66% compared to  $10^{-8}$  M C5a-C5aR interaction. The histamine release from HMC-1 cells induced by  $10^{-8}$  M C5a was apparently not changed in the presence of  $10^{-7}$  M C5a/RP S19. This potency seemed to be a sum of the competitive potency of C5a/RP S19 against C5a at the receptor level and the agonistic potency of C5a/RP S19. These results indicate that C5a/RP S19 could trigger an alternative PI3K pathway, distinct from

the canonical PLC $\beta$ 2-PI3K pathway that is activated by the C5a-C5aR interaction.

Similar results were also observed in the chemotaxis chamber assay. C5a attracted HMC-1 cells, resulting in a sharp bell-shaped dose-response curve with an optimal dose of  $10^{-8}$  M (Fig. 1D). Although C5a/RP S19 also attracted HMC-1 cells, the intensity was low, with an optimal concentration of  $10^{-7}$  M. As in the case of the C5a-induced reaction, the C5a/RP S19-induced chemotaxis was not modified neither by the C3aR blockade nor by the C5L2 blockade, whereas it was suppressed by any one of the C5aR blockade (Fig. 1E). These data confirmed that the HMC-1 cell migration against C5a/RP S19 was a C5aR-mediated reaction. In the case of the chemotactic response induced by  $10^{-8}$  M C5a, the apparent antagonist-induced effect of C5a/RP S19 was obvious at concentrations as high as  $10^{-7}$  M and  $10^{-6}$  M (Fig. 1F). These results suggest that  $10^{-6}$  M C5a/RP S19 may almost completely dissociate  $10^{-8}$  M C5a from the C5aR on HMC-1 cells.

#### Comparison of C5a and C5a/RP S19 binding to C5aR

We re-examined the binding affinity of C5a/RP S19 for C5aR on HMC-1 cells that had been previously shown in neutrophils [19]. We prepared synthetic peptides with C-terminal additions (YSFKDMQLGR and YSFKDMQLDRIAGQVAAANKKH) in order to mimic the second binding motifs of C5a and C5a/RP S19, respectively [14]. As shown in Fig. 2A, while these peptides competed almost equally with the  $^{125}$ I-labeled C5a peptide in the binding assay at lower concentrations, the C5a/RP S19 peptide demonstrated a stronger competition capacity than did the C5a peptide at higher concentrations, such as  $10^{-5}$  M. The difference was small but significant and reproducible. We re-plotted these competition curves in a logarithmic-logarithmic manner and calculated the apparent binding affinities of C5a and C5a/RP S19 for C5aR from their slopes at high concentrations. The apparent binding affinity of the C5a/RP S19 peptide [ $y=-3055.6\ln(x)+10308$ ,  $R^2=0.9923$ ] was 1.6 times higher than that of the C5a peptide [ $y=-1891.5\ln(x)+8834.1$ ,  $R^2=0.9853$ ] (Fig. 2C), as had been previously shown in neutrophils [20]. Our results indicated that, at higher concentrations, the binding affinity of the IAGQVAAANKKH peptide is 60% higher for C5aR than the baseline affinity.

We confirmed the better binding affinity of C5a/RP S19 than C5a to C5aR using the recombinant proteins. In this experiment, the amount of binding of  $^{125}$ I-labeled C5a protein to HMC-1 cells was quantified under the presence of either unlabeled C5a or unlabeled C5a/RP S19 at various concentrations (Fig. 2D). We then obtained the concentration of each unlabeled protein to inhibit the radio-labeled C5a down to 50 percent as  $IC_{50}$ ;  $IC_{50}=10^{\log(\frac{\text{unlabeled ligand concentration to express the higher inhibition than 50\%}}{\text{unlabeled ligand concentration to express the lower inhibition than 50\%}} \times (50\% - \frac{\text{higher inhibition than 50\%}}{\text{lower inhibition than 50\%}}) / (\frac{\text{higher inhibition than 50\%}}{\text{lower inhibition than 50\%}} + \log(\frac{\text{unlabeled ligand concentration to express the lower inhibition than 50\%}}{\text{unlabeled ligand concentration to express the higher inhibition than 50\%}}))$ . The apparent  $IC_{50}$  of C5a/RP S19 to the C5a-C5aR interaction ( $2.2 \times 10^{-8}$  M) was 2.5 times less than that of C5a ( $5.4 \times 10^{-8}$  M). Importantly, the binding of  $^{125}$ I-labeled C5a to HMC-1 cells was not modified by the C3aR blockade, SB-290157, whereas it was suppressed either by the C5aR blockades such as PMX-53, W-54011, and anti-C5aR rabbit IgG or by the C5L2 blockade, anti-C5L2 goat IgG, respectively (Fig. 2E).

The blocking with anti-C5L2 goat IgG was more efficiently observed in the C5a/RP S19 binding than in the C5a binding. These data indicate that C5a/RP S19 binds not only to the C5aR but also to the C5L2 at least on HMC-1 cells. To purely compare the binding affinity to C5aR between C5a and C5a/RP S19, we initially treated HMC-1 cells with anti-C5L2 goat IgG to block C5L2, then mixed the cells either with the  $^{125}$ I-labeled C5a protein or with the  $^{125}$ I-labeled C5a/RP S19 protein in the presence of various concentrations of PMX-53, the most effective C5aR antagonist, and finally obtained  $IC_{50}$  concentrations of PMX-53 (Fig. 2F). The apparent  $IC_{50}$  of PMX-53 to the C5a/RP S19-C5aR interaction ( $7.2 \times 10^{-8}$  M) was 1.8 times higher than that to the C5a-C5aR interaction ( $4.0 \times 10^{-8}$  M). These data confirmed that the binding affinity of C5a/RP S19 to the C5aR was significantly higher than that of C5a.

#### Different C5aR agonist-induced effects on cytoplasmic $Ca^{2+}$ influx observed with C5a and C5a/RP S19

The fact that C5a/RP S19 has stronger binding affinity for C5aR than C5a suggests that these proteins may each trigger  $Ca^{2+}$  mobilization through different Gi protein-dependent pathways. We compared cytoplasmic  $Ca^{2+}$  influx upon the binding of C5aR to C5a or with C5a/RP S19 in HMC-1 cells. C5a induced a cytoplasmic  $Ca^{2+}$  influx at concentrations from  $10^{-9}$  M and upward, showing a plateau at  $10^{-8}$  M (Fig. 3A). In contrast, C5a/RP S19 also induced an influx, but only at concentrations of  $10^{-7}$  M or higher (Fig. 3A). These

data reflect the different responses stimulated by C5a and C5a/RP S19 (Fig. 1A, 1D). An interesting observation is that the increase in cytoplasmic  $\text{Ca}^{2+}$  lasted longer during the C5a/RP S19 stimulation. This result suggests that the desensitization pathway and/or the calcium channels induced by C5aR may be different for C5a and C5a/RP S19.

It is commonly thought that, upon Gi protein-dependent signaling,  $\text{Ca}^{2+}$  enters the cytoplasm from intracellular pools, such as those found in the endoplasmic reticulum (ER) and the extracellular space [2]. Considering the low  $\text{Ca}^{2+}$  response to C5a/RP S19, we hypothesized that one of these modes of  $\text{Ca}^{2+}$  influx might be impaired when this ligand is bound. To clarify this, we examined the effect of extracellular  $\text{Ca}^{2+}$  removal on the cytoplasmic  $\text{Ca}^{2+}$  influx observed upon the binding of C5a/RP S19 or C5a to the C5aR. As shown in Fig. 3A-B,  $10^{-7}$  M C5a/RP S19-induced cytoplasmic  $\text{Ca}^{2+}$  influx almost completely disappeared when  $\text{Ca}^{2+}$ -free, 2 mM EGTA-containing medium was used during the stimulation of HMC-1 cells. In the case of  $10^{-8}$  M C5a-induced cytoplasmic  $\text{Ca}^{2+}$  influx, about one third of the total influx remained, even in the absence of extracellular  $\text{Ca}^{2+}$ . The remaining influx, observed upon stimulation with  $10^{-8}$  M C5a, was completely abrogated by the simultaneous addition of  $10^{-7}$  M C5a/RP S19 (Fig. 3C). These data indicate that receptor competition may occur, at least in part, due to an antagonistic mechanism. The C5aR competition-induced effect of  $10^{-8}$  M C5a/RP S19 was observed again when C5a and C5a/RP S19 were used in combination at equal concentrations (Fig. 3D).

Based on these results and the published literature [33], one could predict that PLC $\beta$ 2 activation may be, at least in part, blocked upon the ligation of C5a/RP S19 to the C5aR in HMC-1 cells, resulting in the inhibition of intracellular  $\text{Ca}^{2+}$  release from the ER *via* IP3R and the ryanodine receptor (RyR). In this case, a  $\text{Ca}^{2+}$  channel other than CRAC on the plasma membrane may allow the entry of extracellular  $\text{Ca}^{2+}$ .

#### Lack of C5aR desensitization upon ligation with C5a/RP S19

It has been previously determined that C5aR is internalized upon ligation with C5a and that this inhibits  $\text{Ca}^{2+}$  influx. For ligand-induced internalization of C5aR, the phosphorylation of serine residues at the C-terminal intracellular region and subsequent binding by arrestin are essential. Phosphorylation of these serine residues is sequentially catalyzed by protein kinase C (PKC) and G protein-coupled receptor kinase 2 (GRK2) downstream of PLC $\beta$ 2 [33-35]. We predicted that C5aR internalization would not occur if the PLC $\beta$ 2 pathway was negligibly involved in the intracellular signal transduction mediated by the agonist-induced effect of C5a/RP S19, as described above. We tested this prediction experimentally with FACS analysis. As shown in Fig. 4A, while the number of HMC-1 cells expressing C5aR on their surface was significantly decreased by 10 min after the treatment with  $10^{-8}$  M C5a, C5aR remained on the cell surface for at least 30 min after treatment with  $10^{-7}$  M C5a/RP S19. Furthermore, C5aR internalization induced by  $10^{-8}$  M C5a was significantly inhibited by the simultaneous presence of  $10^{-7}$  M C5a/RP S19, as shown in our chemotaxis assay (Fig. 1E). The incomplete C5aR internalization is consistent with the long-lasting cytoplasmic  $\text{Ca}^{2+}$  increase that we observed as an agonist-induced effect of C5a/RP S19 (Fig. 3A).

#### Different intracellular signal transduction pathways are regulated by C5a and C5a/RP S19

It is known that C5aR preferentially interacts with the G $\alpha$ i2 subunit of the G $\alpha$  subunit family and that both the G $\alpha$ i2 and G $\beta$  $\gamma$  subunits phosphorylate PKB (Akt) downstream of PI3K and ERK1/2 downstream of PLC $\beta$ 2 with similar activities [2, 36]. We examined Akt and ERK1/2 phosphorylation by western blot. As shown in Fig. 4B and Supplemental Fig. 3, when HMC-1 cells were stimulated with  $10^{-8}$  M C5a, phosphorylation of both Akt and ERK1/2 were observed for a relatively long period of time (30 min). When the cells were stimulated with  $10^{-7}$  M C5a/RP S19, phosphorylation of both proteins was observed, but was significantly weaker and lasted for only 10 min. When the cells were stimulated with a mixture of  $10^{-8}$  M C5a and  $10^{-7}$  M C5a/RP S19, only the C5a/RP S19-induced pattern was observed. These results suggest that the usual Gi protein-dependent signal pathway modulated by the C5a/RP S19-C5aR interaction were different from the canonical pathway regulated by the C5a-C5aR interaction.

Consequently, this result indicated that there could be an alternative activation of a MAPK module(s) other than ERK1/2 upon C5a/RP S19-C5aR interaction. Among the other two MAPK subgroups, p38MAPK is well documented to have a pro-apoptotic function [37, 38]. Considering the pro-apoptotic effect of the C5a/RP S19-C5aR interaction on apoptosis-initiated cells as a result of decreased ERK1/2 phosphorylation

[20], we thought that p38MAPK might be involved in the C5a/RP S19-induced response of HMC-1 cells, although the coupling between Gi protein-coupled receptors (GiPCRs) and p38MAPK has not been well described [39]. Interestingly, p38MAPK was reported to be inhibited by GRK2 due to phosphorylation at Thr123 on the docking groove of p38MAPK. This groove is essential for interactions with the activator MAPK-kinase 6 and with substrates of p38MAPK [40]. The incomplete C5aR internalization upon ligation to C5a/RP S19 described above strongly suggested that GRK2 was incompletely activated, which in turn suggested that p38MAPK was activated. We examined the activation-specific phosphorylation state of p38MAPK using anti-Thr180/Tyr182 dual phospho-p38MAPK rabbit IgG before and after stimulation with  $10^{-7}$  M C5a/RP S19. As shown in Fig. 4C, phosphorylation of p38MAPK was clearly caused by C5a/RP S19 stimulation. It is well known that the activation of p38MAPK is often associated with JNK activation [39]. As might be expected, JNK phosphorylation was observed, in addition to weak ERK1/2 phosphorylation.

All of the above data lead us to speculate that the binding of the C-terminus of RP S19 (I<sub>134</sub>-H<sub>145</sub>) to C5aR could activate p38MAPK, as well as simultaneously suppress direct PI3K activation upstream of Akt and indirect PI3K activation driven from PLC $\beta$ 2 upstream of ERK1/2. Because we have not observed a direct interaction between the RP S19 dimer or C5a/RP S19 and the Gi protein, a modulator for inhibiting the dissociation of the trimeric Gi protein must be discussed. We assume that some Gi protein-dependent pathways are activated by the RP S19 dimer, and are responsible for the weak direct activation of PI3K and the indirect activation of PI3K driven from PLC $\beta$ 2.

#### Pharmacological regulation of the alternative p38MAPK pathway

If our above speculation was correct, we should be able to artificially induce the pathway initiated by the C5a/RP S19-C5aR interaction with C5a by pharmacologically blocking the activation of both PI3K and PLC. To this end, HMC-1 cells pre-treated with specific inhibitors for PLC (U73122) and/or PI3K (LY294002) were stimulated with  $10^{-8}$  M C5a, and p38MAPK phosphorylation was analyzed by western blot. As shown in Fig. 5A, neither U73122 nor LY294002 alone could convert the C5a-induced signal pathway to the C5a/RP S19-induced pathway. However, the combined use of U73122 and LY294002 resulted in p38MAPK phosphorylation upon C5a-C5aR interaction, although it was not as strong as that observed upon the C5a/RP S19-C5aR interaction. Conversely, the alternative p38MAPK phosphorylation pattern derived from C5a/RP S19-C5aR interaction was lost upon the over-stimulation of PKC with  $10^{-8}$  M PMA (Fig. 5A).

If this p38MAPK phosphorylation occurred due to the alternation of the PLC $\beta$ 2 pathway, we should observe long lasting intra-cytoplasmic Ca<sup>2+</sup> influx due to a lack of C5aR internalization. As shown in Fig. 5B-C, in the presence of both U73122 and LY294002, Ca<sup>2+</sup> influx became weaker but lasted longer and C5aR internalization was reduced, although the alternation of the signaling pathway was incomplete. To confirm whether the RP S19 dimer activated the same signal transduction pathway in HMC-1 cells as did C5a/RP S19, the phosphorylation states of Akt and p38MAPK were evaluated by western blotting after stimulation with  $10^{-8}$  M RP S19 dimer (Fig. 5D). Importantly, the RP S19 dimer predominantly stimulated the alternative p38MAPK pathway at the same concentration of C5a.

#### Different calcium mobilization loops are stimulated by C5a versus C5a/RP S19 binding to C5aR

To identify a calcium channel within the plasma membrane that could be involved in the alternative C5a/RP S19-C5aR-PLC $\beta$ 2-p38MAPK-PI3K pathway, we used a variety of pharmacological agents to modify the Ca<sup>2+</sup> signals sent by C5a and by C5a/RP S19. We used an inhibitor of Gai/o proteins (PTX), an ERK inhibitor (PD98059), a p38MAPK inhibitor (SB203580), phospholipase A<sub>2</sub> (PLA<sub>2</sub>), a PLA<sub>2</sub>-dependent transient receptor potential (TRP) inhibitor (ACA), another TRP inhibitor (Ruthenium Red), and a CRAC inhibitor (2-APB). HMC-1 cells were pretreated with one inhibitor for 60 min before stimulation with  $10^{-8}$  M C5a or  $10^{-7}$  M C5a/RP S19. The resulting cytoplasmic Ca<sup>2+</sup> influx was measured in the usual Ca<sup>2+</sup>-containing medium. Results are shown in Fig. 6A. Both of the cytoplasmic Ca<sup>2+</sup> influxes were completely inhibited by PTX, indicating that the C5aR-Gai2 $\beta$  $\gamma$  interaction could initiate signaling upon the interaction of C5a/RP S19 and C5aR. Differences in the patterns of inhibition of cytoplasmic Ca<sup>2+</sup> influx caused by C5a and by C5a/RP S19 were obvious when we used 2-APB, ACA, or SB20358. The higher sensitivity of C5a to 2-APB reflects the participation of intracellular Ca<sup>2+</sup> from the ER, and the higher sensitivity of C5a/RP S19 to ACA and SB20358 reflects that its source of Ca<sup>2+</sup> is only from the extracellular space. In both cases, calcium mobilization was also completely blocked by PD98059, indicating that the complete loss of GRK2-induced

desensitization of C5aR did not affect downstream signal transduction pathways. Consistent with these results, not only ERK but also p38MAPK phosphorylation was suppressed by PD98059 (Fig. 6B). Importantly, although an upregulation of p38MAPK phosphorylation by a low concentration of specific inhibitors for PLC (U73122) and PI3K (LY294002) was observed upon C5a-C5aR interaction (Fig. 5A), the same concentration of LY294002 specifically blocked p38MAPK phosphorylation upon C5a/RP S19-C5aR interaction without affecting the ERK phosphorylation (Fig. 6B). This confirms the requirement of weak PLC $\beta$ 2 and PI3K activation upstream of the extracellular Ca<sup>2+</sup> entry (Fig. 5B).

The data indicated that the main extracellular Ca<sup>2+</sup> gate is an ACA-sensitive TRP. TRP subfamilies, including members of the melastatin (TRPM), vanilloid, and canonical families, have been implicated in Ca<sup>2+</sup> signaling [39]. Recently, TRPM2 and TRPM8, which are sensitive to PLA<sub>2</sub> and ACA, were reported to be inhibited by Mg<sup>2+</sup> [41]. Thus, we examined the sensitivity of C5a/RP S19-C5aR interaction-induced extracellular Ca<sup>2+</sup> entry to extracellular Mg<sup>2+</sup> concentration. As shown in Fig. 6C, the cytoplasmic Ca<sup>2+</sup> influx caused by C5a/RP S19, but not by C5a, was greatly reduced by the presence of MgCl<sub>2</sub> in a concentration-dependent manner. This strongly suggests that the PM calcium channel downstream of the C5a/RP S19-C5aR-PLC $\beta$ 2/PI3K-p38MAPK pathway is a PLA<sub>2</sub>-sensitive TRPM.

A positive feedback loop between p38MAPK and TRPM in the C5a/RP S19-C5aR signaling pathway

The PLC $\beta$ 2-dependent pathway contains a system for the amplification of cytoplasmic Ca<sup>2+</sup> influx; i.e., a positive feedback loop exists between PKC and intracellular/extracellular Ca<sup>2+</sup> mobilization *via* IP<sub>3</sub>R on the ER and CRAC on the plasma membrane [33]. In contrast, a negative feedback system is also present to prevent excessive biological response. C5aR internalization is ubiquitously induced in all cell types. Therefore, the C5a-C5aR interaction promotes fast and strong Gi protein-dependent signaling (Fig. 4A, 5C). In the current study, we found another positive feedback loop for cytoplasmic Ca<sup>2+</sup> influx. As described above, the inhibition of p38MAPK with SB203580 significantly reduced the cytoplasmic Ca<sup>2+</sup> influx (Fig. 6A). As shown in Fig. 6D, the blockade of cytoplasmic Ca<sup>2+</sup> entry *via* TRAM in the presence of 2.5 mM MgCl<sub>2</sub> greatly attenuated the phosphorylation of both p38MAPK and JNK in the context of C5aR activation by 10<sup>-7</sup> M C5a/RP S19, and *vice versa*. We suspected that the prolonged activation of another positive feedback loop induced by the delay of C5aR internalization would support the accumulation of extracellular Ca<sup>2+</sup> in the cytoplasm of HMC-1 cells.

Ca<sup>2+</sup> signaling, chemotaxis, and histamine release

We confirmed that the feedback loop involving p38MAPK, PLA<sub>2</sub>, and TRAM that causes cytoplasmic Ca<sup>2+</sup> influx was also responsible for C5a/RP S19-induced chemotaxis and histamine release using the inhibitors described above (Fig. 7). Almost complete agreement was observed between cytoplasmic Ca<sup>2+</sup> influx and chemotaxis induced by C5a/RP S19 or by C5a, whereas the inhibition patterns were different in C5a/RP S19 and C5a (Fig. 7A-C). As shown in Fig. 7D-F, the histamine release reaction caused by either C5a or by C5a/RP S19 had a tendency to resist the Ca<sup>2+</sup> channel blocker and removal of extracellular Ca<sup>2+</sup>. These results indicate that the upstream signal for activating the TRPM is enough to induce almost the full index of histamine release, while the downstream Ca<sup>2+</sup> signal is required for the full index of chemotaxis.

From the above data, we conclude that when the C5aR on HMC-1 cells is engaged by the additional binding of the C-terminus of RP S19 (I<sub>134</sub>-H<sub>145</sub>), PLC $\beta$ 2 and PI3K are weakly activated by the Gi protein (Fig. 8B). However, this weak activation of PI3K is not enough to directly induce chemotaxis and histamine release; the indirect activation of PI3K driven from PLC $\beta$ 2 and PI3K is required for the initiation of biological responses. Incomplete C5aR sensitization and the positive feedback loop between p38MAPK and TRPM are involved in the alternative PI3K pathway.

## Discussion

Here, we propose a possible mechanism for initiation of a trimeric G $\alpha$ i2 $\beta$  $\gamma$  protein-dependent alternative PI3K pathway *via* C5aR. Although the Gi protein-dependent p38MAPK pathway activated by C5a/RP S19 is usually blocked not only by the activation of PKB but also the inhibition of adenylate cyclase [3], we found that when this pathway was partially blocked by the combinatory use of the inhibitors U73122 and LY294002 at relatively low concentrations (2  $\mu$ M), C5aR stimulates an alternative p38MAPK pathway (Fig.

5A). In contrast, the trimeric Gi protein-dependent alternative activation of p38MAPK triggered by C5a/RP S19 was blocked by the use of the PI3K inhibitor LY294002 at relatively low concentrations (2  $\mu$ M) (Fig. 6B). In addition to this, p38MAPK activation was also regulated by the over-stimulation of PKC and the inhibition of ERK activation downstream of the Gi protein (Fig. 5A and 6B). In the context of the previously published literature [42], our results indicate that this p38MAPK activation is regulated by both the Gi protein and incomplete C5aR desensitization (Fig. 8B).

We have demonstrated that the RP S19 dimer derived from apoptotic cells supports the phagocytic clearance of apoptotic bodies by attracting macrophages [5]. Interestingly, although the C5aR on both macrophages and neutrophils is accepted by the RP S19 dimer, neutrophils are not responsible for the clearance, and it is very important to determine why only macrophages find apoptotic bodies. We have found a novel PI3K pathway that is activated *via* the C5aR on HMC-1 cells that involves a positive feedback loop between p38MAPK and TRPM to accumulate cytoplasmic  $Ca^{2+}$  in order to promote remodeling of the actin cytoskeleton [43]. We believe that the alternative pathway is, at least in part, common not only in mast cells (Supplemental Fig. 1-2), but also in macrophages (Supplemental Fig. 4). It is worth examining whether the canonical and alternative signal pathways stimulated by C5aR in HMC-1 cells are used to achieve opposing outcomes in macrophages and neutrophils.

Since we demonstrated the presence of the apoptotic cell-derived RP S19 dimer, at least three kinds of chemoattractants have been reported [44-46]. However, the real contribution of their receptors to apoptosis *in vivo* is not well understood. It is particularly interesting that three of the four receptors described in these papers are G protein-coupled. In addition to the RP S19 dimer, thrombospondin-1 (TSP-1) also binds to GiPCR. In this case, the pertussis toxin (PTX)-sensitive Gi protein-dependent intracellular signal transduction pathway was strongly inhibited by a PKC activator, PMA, and activated by a PKC inhibitor, calphostin C. This report indicates the presence of the weakly activated PMA-induced pathway, as shown in Figure 5A.

The precise molecular mechanism underlying the inhibition of canonical signal pathways by the C-terminus of RP S19 (I<sub>134</sub>-H<sub>145</sub>) is still obscure, although it is clear that the 12 additional residues contribute to its inhibitory function. One possibility is that the inhibition depends on a direct binding of I<sub>134</sub>-H<sub>145</sub> to Gi protein or both PLC and PI3K. However, we have not found direct evidence for these interactions (data not shown). Therefore, we are now very interested in identifying modulators that may suppress the Gi protein or both PLC and PI3K activation after interacting with I<sub>134</sub>-H<sub>145</sub>. Another possibility is that the inhibition depends on different conformational changes of the C5aR on HMC-1 cells than those stimulated by C5a [2]. We have observed that deletion of two amino acid residues (Lys<sub>144</sub>His<sub>145</sub>) at the C-terminus of a RP S19-mimicking peptide resulted in a loss of the C5aR competition-induced function [13], suggesting that the interaction of the Lys residue with a part of C5aR, or with a molecule other than C5aR, may be causing the real inhibition.

One of the most interesting aspects of the alternative PI3K pathway is its sole use of extracellular  $Ca^{2+}$  *via* TRPM (Fig. 3A, 5B, 6A, and 6C). The cytoplasmic  $Ca^{2+}$  influx was blocked by the PLA<sub>2</sub> inhibitor ACA (Fig. 6A). These results indicate that TRPM in this pathway is activated by arachidonic acid-derived eicosanoids, as reported previously [47]. It has also been reported that TRPM2, 5, 7, and 8 were activated by arachidonic acid [48-51]. Therefore, TRPM2 and M7 would be good candidate gatekeepers for extracellular  $Ca^{2+}$  entry into mast cells. This pathway is strikingly different from the PLC $\beta$ 2-dependent signal transduction pathway that is activated upon the C5a-C5aR interaction (Fig. 8). We confirmed the influx of extracellular  $Ca^{2+}$  *via* CRAC on the PM in addition to the ER-derived  $Ca^{2+}$  (Fig. 6A) [33]. The activation of p38MAPK caused a cytoplasmic  $Ca^{2+}$  influx *via* TRPM, and the  $Ca^{2+}$  signal, in turn, augmented p38MAPK phosphorylation (Fig. 6D). This pathway does not stimulate complete C5aR internalization, which results in receptor desensitization (Fig. 4A and 5C). The alternative activation of a positive feedback loop with incomplete receptor internalization resulted in a weak but prolonged cytoplasmic  $Ca^{2+}$  influx (Fig. 3A, 5B) and subsequent induction of histamine release and chemotaxis (Fig. 7) [52]. The activation of TRPM by cytoplasmic  $Ca^{2+}$  was also reported for a TRPM member, TRPM5 [50]. This positive feedback loop causes cytoplasmic  $Ca^{2+}$  accumulation for a long period and eventually triggers final cellular events, such as taste sensing.

G protein-uncoupled C5L2 is coexpressed with the C5aR at least on monocytes and granulocytes [2, 53].

Although C5L2 is known to accept not only C5a and desarginated C5a but also C3a and desarginated C3a [54], C5L2-mediated effect is not known [55]. In contrast to C5aR, C5L2 lacks the serine residues at the C-terminal region important for binding to arrestin and for selection of ERK1/2 in MAPK modules. Therefore, an active form of C5L2 remains on the cell surface. HMC-1 cells are already known to express high levels of both C5L2 and C5aR [56]. C5a/RP S19 binds not only to the C5aR but also to C5L2 (Fig. 2E). However, the histamine release and chemotaxis of HMC-1 induced by either C5a or C5a/RP S19 were not modified by the anti-C5L2 goat IgG (Fig. 1B and 1E). We separately examined a possibility that the C5a/RP S19-C5L2 interaction might be involved in the exchange of MAPK module from ERK1/2 to p38MAPK downstream of the C5aR on HMC-1 cells (Fig. 4B and 5A). However, the C5a/RP S19-guided selection of p38MAPK was not cancelled by the anti-C5L2 goat IgG (data not shown). These data suggest that the C5L2 on HMC-1 cells works as a decoy receptor.

We have elucidated a common mechanism underlying the opposing C5aR agonist-induced functions in apoptosis-initiated cells. Pro-apoptotic processes are mediated by the C5a/RP S19-C5aR interaction, and anti-apoptotic processes are mediated by the C5a-C5aR interaction [19]. In the former pro-apoptotic effect, enhanced gene expression of regulator of G protein signaling 3 is essential [20]. We observed the suppression of ERK phosphorylation and C5aR desensitization upon C5a/RP S19-C5aR interaction, even in HMC-1 cells (Fig. 4, 5C-D). Although the apoptosis-related effect is long term and different from other effects, such as chemotaxis and granule release, it will be worth examining whether the canonical and alternative C5aR signal pathways that have been revealed in HMC-1 apoptosis-initiated cells are used to produce opposing apoptotic outcomes [57].

## **Acknowledgments**

This work was supported by Japan Science and Technology Agency (project code: 09801156) and a Grant-in-Aid for Scientific Research (C) (KAKENHI 22590362) from the Ministry of Education, Culture, Sports, Science, and Technology, Japan.

## References

1. Gerard NP, Bao L, Xiao-Ping H, Eddy RL Jr, Shows TB, Gerard C (1993) Human chemotaxis receptor genes cluster at 19q13.3–13.4. Characterization of the human C5a receptor gene. *Biochemistry* 32:1243–1250
2. Monk PN, Scola A-M, Madala P, Fairlie DP (2007) Function, structure and therapeutic potential of complement C5a receptors. *Br J Pharm* 152:429–448
3. Goldsmith ZG, Dhanasekaran DN (2007) G Protein regulation of MAPK networks. *Oncogene* 26:3122–3142
4. Siciliano SJ, Rollins TE, DeMartino J, Konteatis Z, Malkowitz L, Van, RG, Bondy S, Rosen H, Springer MS (1994) Two-site binding of C5a by its receptor: an alternative binding paradigm for G protein-coupled receptors. *Proc Natl Acad Sci USA* 91:1214-1218
5. Yamamoto T (2007) Roles of the ribosomal protein S19 dimer and the C5a receptor in pathophysiological functions of phagocytic leukocytes. *Pathol Int* 57:1-11
6. Nishiura H, Shibuya Y, Matsubara S, Tanase S, Kambara T, Yamamoto T (1996) Monocyte chemotactic factor in rheumatoid arthritis synovial tissue: probably a cross-linked derivative of S19 ribosomal protein. *J Biol Chem* 271:878-882
7. Shrestha A, Shi L, Tanase S, Tsukamoto M, Nishino N, Tokita K, Yamamoto T (2004) Bacterial chaperone protein, Skp, induces leukocyte chemotaxis via C5a receptor. *Am J Pathol* 164:763-72
8. Nishiura H, Tanase S, Shibuya Y, Nishimura T, Yamamoto T (1999) Determination of the cross-linked residues in homo-dimerization of S19 ribosomal protein concomitant with exhibition of monocyte chemotactic activity. *Lab Invest* 79:915-923
9. Horino K, Nishiura H, Ohsako T, Shibuya Y, Hiraoka T, Kitamura N, Yamamoto T (1998) A monocyte chemotactic factor, S19 ribosomal protein dimer, in phagocytic clearance of apoptotic cells. *Lab Invest* 78:603-617
10. Nishimura T, Horino K, Nishiura H, Shibuya Y, Hiraoka T, Tanase S, Yamamoto T (2001) Apoptotic cells of an epithelial cell line, AsPC-1, release monocyte chemotactic S19 ribosomal protein dimer. *J Biochem* 129:445-454
11. Shrestha A, Horino K, Nishiura H, Yamamoto T (1999) Acquired immune response as a consequence of the macrophage-dependent apoptotic cell clearance and role of the monocyte chemotactic S19 ribosomal protein dimer in this connection. *Lab Invest* 79:1629-1642
12. Shibuya Y, Shiokawa M, Nishiura H, Nishimura T, Nishino N, Okabe H, Takagi K, Yamamoto T (2001) Identification of receptor binding sites of monocyte chemotactic S19 ribosomal protein dimer. *Am J Pathol* 159:2293-2301
13. Shrestha A, Shiokawa M, Nishimura T, Nishiura H, Tanaka Y, Nishino N, Shibuya Y, Yamamoto T (2003) Switch moiety in agonist/antagonist dual effect of S19 ribosomal protein dimer on leukocyte chemotactic C5a receptor. *Am J Pathol* 162:1381-1388
14. Nishiura H, Shibuya Y, Yamamoto T (1998) S19 ribosomal protein cross-linked dimer causes monocyte-predominant infiltration by means of molecular mimicry to complement C5a. *Lab Invest* 78:1615-1623
15. Revollo I, Nishiura H, Shibuya Y, Oda Y, Nishino N, Yamamoto T (2005) Agonist and Antagonist Dual Effect of the Cross-linked Ribosomal Protein Dimer in the C5a Receptor-Mediated Respiratory Burst Reaction of Phagocytic Leukocytes. *Inflam Res* 54:82-90

16. Fukuoka Y, Ember JA, Yasui A, Hugli TE (1998) Cloning and characterization of the guinea pig C5a anaphylatoxin receptor: interspecies diversity among the C5a receptors. *Int Immunol* 10:275-283
17. Umeda, Y, Shibuya Y, Semba U, Tokita K, Nishino N, Yamamoto T 2004 Guinea pig ribosomal protein as precursor of C5a receptor-directed monocyte-selected leukocyte chemotactic factor. *Inflam Res* 53:623-630
18. Oda Y, Tokita K, Ota Y, Li Y, Taniguchi K, Nishino N, Takagi K, Yamamoto T, Nishiura H (2008) Agonistic and Antagonistic Effects of C5a-Chimera Bearing S19 Ribosomal Protein Tail Portion on the C5a Receptor of Monocytes and Neutrophils, Respectively. *J Biochem* 144:371-381
19. Nishiura H, Tanase S, Shibuya Y, Futa N, Sakamoto T, Higginbottom A, Monk P, Zwirner J, Yamamoto T (2005) S19 ribosomal protein dimer augments metal-induced apoptosis in a mouse fibroblastic cell line by ligation of the C5a receptor. *J Cell Biochem* 94:540-553
20. Nishiura H, Nonaka H, Revollo SI, Semba U, Li Y, Ota Y, Irie A, Harada K, Kehrl HJ, Yamamoto T (2009) Pro- and anti-apoptotic dual functions of the C5a receptor: involvement of regulator of G protein signaling 3 and extracellular signal-regulated kinase. *Lab Invest* 89:676-694
21. Gonzalez VM, Fuertes MA, Alonso C, Perez JM (2006) Leukotriene B4 receptors BLT1 and BLT2: Expression and function in human and murine mast cells. *J Immunol* 177:3439-3447
22. Harteneck C, Frenzel H, Kraft R (2007) N-(p-amylcinnamoyl)anthranilic acid (ACA): a phospholipase A(2) inhibitor and TRP channel blocker. *Cardiovasc. Drug Rev* 25:61-75
23. Sumichika H, Sakata K, Sato N, Takeshita S, Ishibuchi S, Nakamura M, Kamahori T, Ehara S, Itoh K, Ohtsuka T, Ohbora T, Mishina T, Komatsu H, Naka Y. (2002) Identification of a potent and orally active non-peptide C5a receptor antagonist. *J Biol Chem* 277:49403-49407
24. Robert SA, Dennis L, James JF, Anthony JJ, Mark AT, Wilfried B, Britta S, Andreas K, Karl FE, Russell DC, Anthony CS, J. PH, Gerald M, Keith WW, Jerry LA, William EB, David CU, Ruth RO, Alison MB, Henry MS (2001) Identification of a Selective Nonpeptide Antagonist of the Anaphylatoxin C3a Receptor That Demonstrates Antiinflammatory Activity in Animal Models. *J Immunol* 166:6341-6348
25. Konteatis, Z.D., Siciliano, S.J., Van-Riper, G., Molineaux, C.J., Pandya, S., Fischer, P., Rosen, H., Mumford, R.A., and Springer, M.S. (1994) Development of C5a receptor antagonists: Differential loss of functional responses. *J. Immunol.* 153, 4200-4205
26. Finch AM, Wong AK, Paczkowski NJ, Wadi SK, Craik DJ, Fairlie DP, Taylor SM (1999) Low-molecular-weight peptidic and cyclic antagonists of the receptor for the complement factor C5a. *J Med Chem* 42:1965-1974
27. Laemmli UK (1970) Cleavage of structural proteins during the assembly of the head of bacteriophage T4. *Nature* 227:680-685
28. Kyhse-Andersen J (1984) Electrophoretic transfer of proteins from polyacrylamide to nitrocellulose: a simple apparatus without buffer tank for rapid transfer of proteins from polyacrylamide to nitrocellulose. *J Biochem Biophys Meth* 10:203-209
29. Shore PA (1971) The chemical determination of histamine. *Meth Biochem Anal* 89-97
30. Matsubara S, Yamamoto T, Tsuruta T, Takagi K, Kambara T (1991) Complement C4-derived monocyte-directed chemotaxis-inhibitory factor: A molecular mechanism to cause polymorphonuclear leukocyte-predominant infiltration in rheumatoid arthritis synovial cavities. *Am J Pathol* 138:1279-1291
31. Falk W, Goldwin RH, Leonard EJ (1980) A 48 well micro-chemotaxis assembly for rapid and accurate measurement of leukocyte migration. *J Immunol Meth* 33:239-247

32. Tokita K, Yamamoto T (2004) Differential role of neutrophils and monocytes during subcutaneous plasma extravasation. *Lab Invest* 84:1174-1184
33. Luca M (2006) Intracellular Calcium, Endothelial Cells and Angiogenesis. *Recent Patents on Anti-Cancer Drug Discov* 1:105-119
34. Skokowa J, Ali SR, Felda O, Kumar V, Konrad S, Shushakova N (2005) Macrophages induce the inflammatory response in the pulmonary Arthus reaction through G alpha i2 activation that controls C5aR and Fc receptor cooperation. *J Immunol* 174:3041-3050
35. Elorza A, Sarnago S, Mayor F Jr (2000) Agonist-dependent modulation of G protein-coupled receptor kinase 2 by mitogen-activated protein kinases. *Mol Pharmacol* 57:778-783
36. Schaeffer V, Cuschieri J, Garcia I, Knoll M, Billgren J, Jelacic S, Bulger E, Maier R\_(2007) The priming effect of C5a on monocytes is predominantly mediated by the p38 MAPK pathway. *Shock* 27:623-630
37. Mehta KD, Miller L (1999) Inhibition of stress-activated p38 mitogen-activated protein kinase induces low-density lipoprotein receptor expression. *Trends Cardiovasc Med* 9:201-205
38. Rubinfeld H, Seger R (2005) The ERK cascade: a prototype of MAPK signaling. *Mol Biotechnol* 31:151-174
39. Hilal-Dandan R, Means CK, Gustafsson AB, Morissette MR, Adams JW, Brunton LL, Heller Brown J. (2004) Lysophosphatidic acid induces hypertrophy of neonatal cardiac myocytes via activation of Gi and Rho. *J Mol Cell Cardiol* 36:481-493
40. Peregrin S, Jurado-Pueyo M, Campos MP, Sanz-Moreno V, Ruiz-Gomez A, Crespo P, Mayor F Jr, Murga C (2006) Phosphorylation of p38 by GRK2 at the docking groove unveils a novel mechanism for inactivating p38MAPK. *Current Biology* 16:2042-2047
41. Markus H, Reinold P (1992) Depletion of intracellular calcium stores activates a calcium current in mast cells. *Nature* 355:353-356
42. Pedersen SF, Owsianik G, Nilius B (2005) TRP channels: an overview. *Cell Calcium* 38:233-252
43. Stacey S.W, Peter ND (2006) Signaling pathways mediating chemotaxis in the social amoeba, *Dictyostelium discoideum*. *Eur J Cell Biol* 85:897-904
44. Guo NH, Zabrenetzky SV, Chandrasekaran L, Sipes MJ, Lawler J, Kruttsch CH, Roberts DD (1998) Differential Roles of Protein Kinase C and Pertussis Toxin-sensitive G-binding Proteins in Modulation of Melanoma Cell Proliferation and Motility by Thrombospondin 1. *Cancer Res* 58:3154-3162
45. Wakasugi K, Schimmel P (1999) Two distinct cytokines released from a human aminoacyl-tRNA synthetase. *Science* 284:147-151
46. Peter C, Waibel M, Radu CG, Yang LV, Witte ON, Schulze-Osthoff K, Wesselborg S, Lauber K (2008) Migration to apoptotic "find-me" signals is mediated via the phagocyte receptor G2A. *J Biol Chem* 283:5296-5305
47. Touyz RM (2008) Transient receptor potential melastatin 6 and 7 channels, magnesium transport, and vascular biology: implications in hypertension. *Am J Physiol Heart Circ Physiol* 294:1103-1118
48. Aarts M, Iihara K, Wei WL, Xiong ZG, Arundine M, Cerwinski W, MacDonald JF, Tymianski M (2003) A key role for TRPM7 channels in anoxic neuronal death. *Cell* 115:863-877

49. Zhang IW, Hirschler-Laszkiewicz Q, Tong K, Conrad SC, Sun L, Penn DL, Barber R, Stahl DJ, Carey JY, Cheung BA (2006) TRPM2 is an ion channel that modulates hematopoietic cell death through activation of caspases and PARP cleavage. *Am J Physiol Cell Physiol* 290:1146-1159
50. Oike H, Wakamori M, Mori Y, Nakanishi H, Taguchi R, Misaka T, Matsumoto I, Abe K (2006) Arachidonic acid can function as a signaling modulator by activating the TRPM5 cation channel in taste receptor cells. *Biochim Biophys Acta* 1761:1078-1084
51. Andersson DA, Nash M, Bevan S (2007) Modulation of the cold-activated channel TRPM8 by lysophospholipids and polyunsaturated fatty acids. *J Neurosci* 27:3347-3355
52. Zweifach A, Lewis RS (1995) Rapid inactivation of depletion-activated calcium current (ICRAC) due to local calcium feedback. *J Gen Physiol* 105:209-226
53. Cain SA, Monk PN (2002) The orphan receptor C5L2 has high affinity binding sites for complement fragments C5a and C5a des-Arg(74). *J Biol Chem* 277:7165-7169
54. Kalant D, Cain SA, Maslowska M, Sniderman AD, Cianflone K, Monk PN (2003) The chemoattractant receptor-like protein C5L2 binds the C3a des-Arg77/acylation-stimulating protein. *J Biol Chem* 278:11123-11129
55. Gerard NP, Lu B, Liu P, Craig S, Fujiwara Y, Okinaga S, Gerard C (2005) An anti-inflammatory function for the complement anaphylatoxin C5a-binding protein, C5L2. *J Biol Chem* 280:39677-39680
56. Otto M, Hawlisch H, Monk PN, Müller M, Klos A, Karp CL, Köhl J (2004) C5a mutants are potent antagonists of the C5a receptor (CD88) and of C5L2: position 69 is the locus that determines agonism or antagonism. *J Biol Chem* 279:142-151
57. Gougeon ML, Piacentini M (2009) New insights on the role of apoptosis and autophagy in HIV pathogenesis. *Apoptosis* 14:501-508

## Figure legends

Fig. 1. C5aR agonist-induced effects of C5a/RP S19 on histamine release and chemotaxis of HMC-1 cells. (A, D) In comparison with C5a (white columns and circles), agonistic effects of C5a/RP S19 (black columns and circles) were observed in histamine release and chemotaxis assays. (B, E) For the inhibition assay, indicator HMC-1 cells were pretreated with anti-C5aR rabbit IgG, anti-C5L2 goat IgG, SB-290157, C5aR antagonistic/partial agonistic peptide (C5aRA), PMX-53, or W-54011, respectively. (C, F) In the competition experiment, HMC-1 cells were stimulated with C5a (white columns) in the presence (hatched columns) or absence (black columns) of various concentrations of C5a/RP S19. Results were expressed in the percent ratio of released histamine and the number of migrated HMC-1 cells. Data is expressed as mean  $\pm$  SD (n=4). P values of less than 0.05 between C5a and C5a/RP S19 were considered to indicate statistical significance (P<0.05: \*, P<0.01: \*\*).

Fig. 2. Effect of the C-terminus of RP S19 on the binding of C5a to C5aR on HMC-1 cells. C5aR on HMC-1 cells was competitively bound by  $10^{-7}$  M  $^{125}$ I-labeled peptide mimicking the second binding motif of C5a (YSFKDMLGR) in the presence of various concentrations of the unlabeled C5a-mimicking peptide (the dotted line with open circles) or an unlabeled peptide mimicking a binding motif containing the C-terminus of C5a/RP S19 (YSFKDMLDRIAGVAAANKKH) (the plain line with closed circles). The X-axis ranges up to  $10^{-5}$  M (A), under  $10^{-7}$  M (B), and over  $10^{-7}$  M (C), respectively. (D) C5aR was competitively bound by  $10^{-8}$  M  $^{125}$ I-labeled C5a protein in the presence of various concentrations of the unlabeled C5a protein (the dotted line with open circles) or the unlabeled C5a/RP S19 protein (the plain line with closed circles). (E) For the inhibition assay, indicator HMC-1 cells were pretreated with anti-C5aR rabbit IgG, anti-C5L2 goat IgG, SB-290157, PMX-53, and W-54011, respectively. (F) C5aR was competitively bound by  $10^{-8}$  M  $^{125}$ I-labeled C5a protein (the dotted line with open circles) or C5a/RP S19 protein (the plain line with closed circles) in the presence of anti-C5L2 goat IgG and various concentrations of PMX-53, respectively. After incubation for 60 min on ice, the radioactivity the cells was measured for 2 min in a gamma counter. Data is expressed as mean  $\pm$  SD (n=3).

Fig. 3. Extracellular  $\text{Ca}^{2+}$  entry into the cytoplasm of HMC-1 cells. HMC-1 cells preloaded with Fura2-AM in  $\text{Ca}^{2+}$  medium (A) or in  $\text{Ca}^{2+}$ -free medium (B) were activated by C5a and C5a/RP S19. (C) For the competition experiment in  $\text{Ca}^{2+}$ -free medium, HMC-1 cells were activated by C5a in the presence of C5a/RP S19. The fluorescent intensity is represented as a percent ratio of that observed upon stimulation with C5a. (D) HMC-1 cells were activated by C5a in the presence (hatched columns) or absence (white columns) of C5a/RP S19 at various concentrations. The results were expressed as the fluorescent intensity of cytoplasmic  $\text{Ca}^{2+}$ -Fura2-AM at 10 sec after the stimulation. Data is expressed as mean  $\pm$  SD (n=4).

Fig. 4. Alternative activation of MAPK in HMC-1 cells. (A), HMC-1 cells were collected at 10 min (white columns) or 30 min (black columns) after stimulation with C5a, C5a/RP S19, or a mixture of both. The intensity of PE was measured as the number of C5aR counted by FACS analysis (secondary graph). (B) HMC-1 cells were collected at various time points after stimulation with C5a, C5a/RP S19, or a mixture. Akt and ERK phosphorylation were detected by western blot. (C) HMC-1 cells were collected at 0 (white columns), 5 (black columns), 10 (hatched columns), and 20 min (dotted columns) after stimulation with C5a or C5a/RP S19. MAPK phosphorylation was detected by western blot. The percent phosphorylated protein was determined using NIH Image 1.63 software (secondary graph). Data are expressed as mean  $\pm$  SD (n=4).

Fig. 5. Inhibitory profiles of the Gi protein-dependent p38MAPK pathway in HMC-1 cells. (A) HMC-1 cells pre-incubated with U73122, LY294002, or a mixture was stimulated by C5a. HMC-1 cells were stimulated with C5a/RP S19 and PMA. The p38MAPK phosphorylation was detected by western blot. (B) HMC-1 cells preloaded with Fura2-AM were incubated with PBS, U73122, LY294002, or a mixture and were activated by C5a. (C) HMC-1 cells pre-incubated with PBS, U73122, LY294002, or a mixture were collected at 0 min (white columns) and 10 min after stimulation with C5a (black columns) and C5a/RP S19 (hatched columns), respectively. The intensity of PE was measured as the number of C5aR counted by FACS analysis. Data is expressed as mean  $\pm$  SD (n=4). (D) HMC-1 cells were stimulated by the RP S19 dimer and Akt and p38MAPK phosphorylation was detected by western blot.

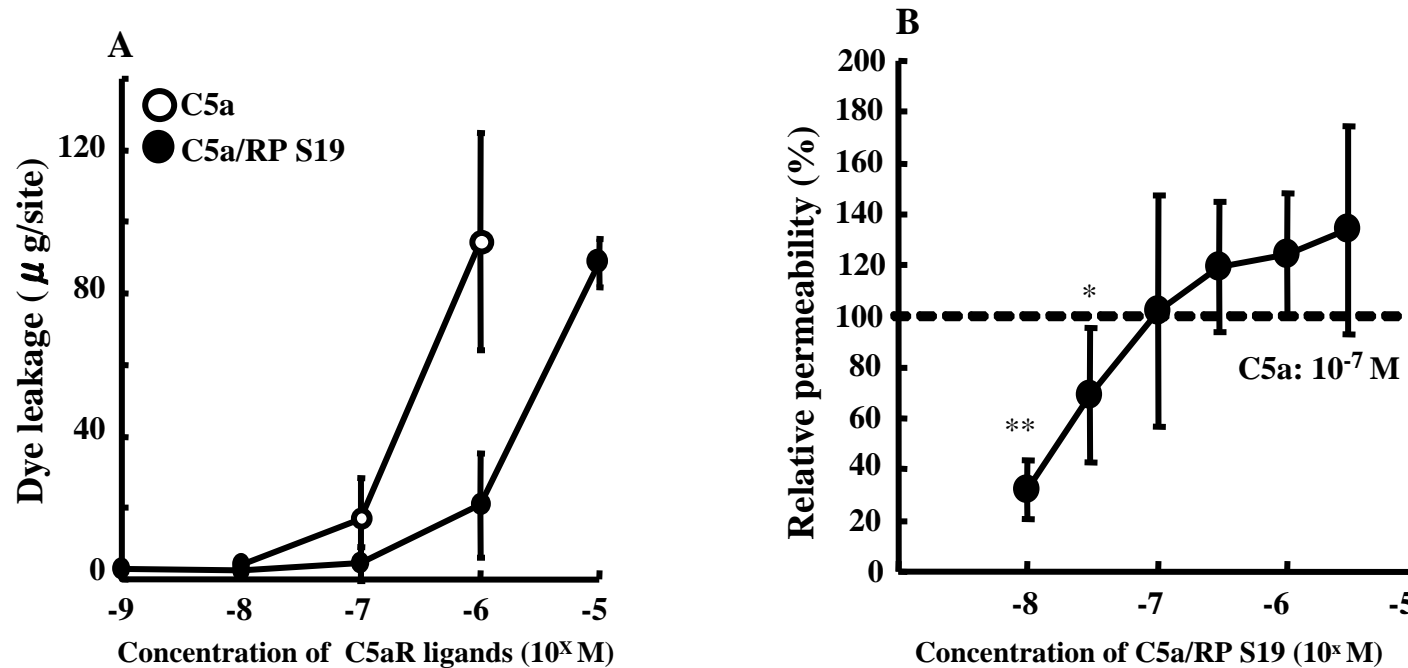
Fig. 6. An alternative positive feedback loop involving p38MAPK and extracellular  $\text{Ca}^{2+}$  entry in HMC-1 cells. (A) HMC-1 cells preloaded with Fura2-AM were incubated with several kinds of inhibitors. The cells

were activated by C5a or C5a/RP S19. The fluorescent intensity is expressed as a percent ratio of that observed without the inhibitor (n=4). (B) HMC-1 cells pre-incubated with inhibitor were collected at several time points after stimulation with C5a/RP S19. ERK and p38MAPK phosphorylation was detected by western blot. (C) HMC-1 cells preloaded with Fura2-AM were activated by C5a, C5a/RP S19, or fMLP in the presence of various concentrations of MgCl<sub>2</sub>. (D) HMC-1 cells were stimulated with C5a/RP S19 in the presence or absence of 2.5 mM MgCl<sub>2</sub>. Akt and MAPK phosphorylation was detected by western blot (n=4). The relative rate of phosphorylated protein to the total protein is expressed in percent.

Fig. 7. Effect of extracellular Ca<sup>2+</sup> entry *via* TRP. (A, D) HMC-1 cells pre-treated with several kinds of inhibitors were activated by 10<sup>-8</sup> M C5a (white columns) or 10<sup>-7</sup> M C5a/RP S19 (black columns) in the chemotaxis chamber or 1.5 ml tubes, respectively. (B, E) HMC-1 cells in Ca<sup>2+</sup> medium or in Ca<sup>2+</sup>-free medium were activated by various concentrations of C5a (white columns) or C5a/RP S19 (black columns). (C, F) HMC-1 cells were activated by C5a (white columns), C5a/RP S19 (black columns), or fMLP (hatched columns) in the presence of various concentrations of MgCl<sub>2</sub>. Results were expressed as the percent ratio of the number of migrated HMC-1 cells and or the amount of histamine released compared to untreated cells. Data is expressed as mean ± SD (n=4).

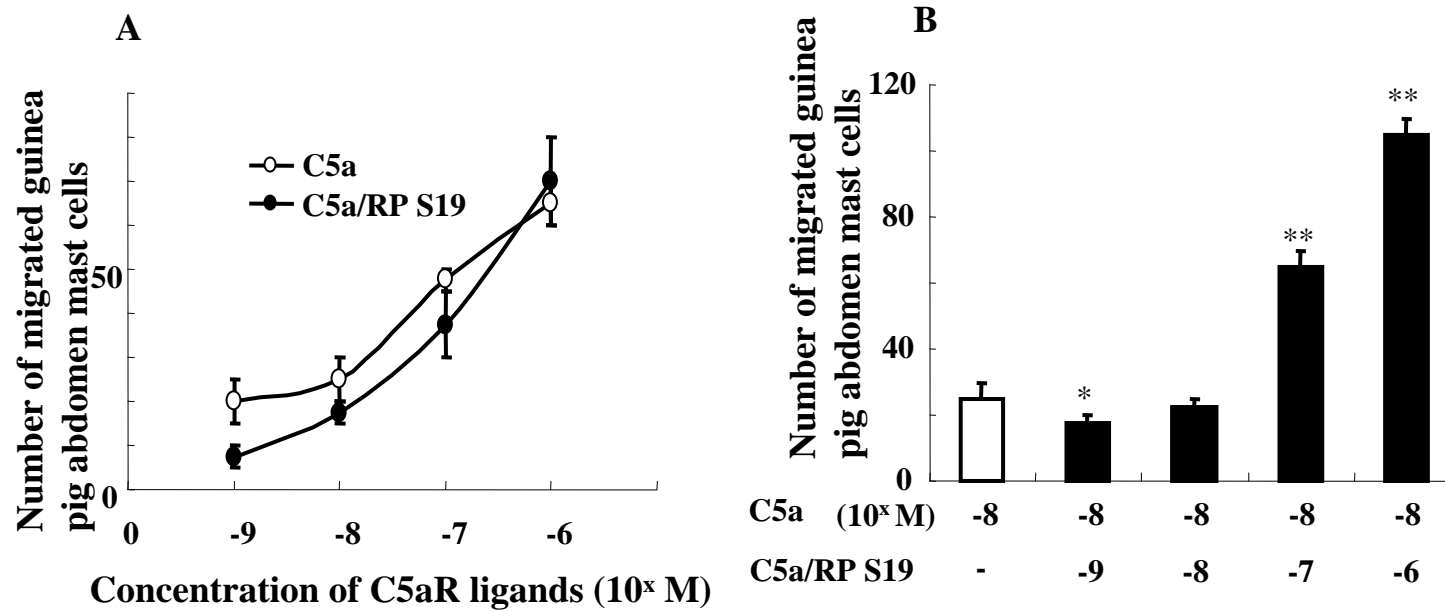
Fig. 8. Schematic representation of different C5aR-mediated Gi protein-dependent PI3K pathways in HMC-1 cells. (A) The Gi protein-dependent canonical PI3K pathway in C5a-C5aR interaction. The PI3K activation is amplified by the positive feedback loop between PI3R and CRAC. (B) The Gi protein-dependent alternative PI3K pathway in the RP S19 dimer-C5aR interaction. The PI3K activation is amplified by the positive feedback loop between p38MAPK and TRPM.

## Supplemental Figure 1



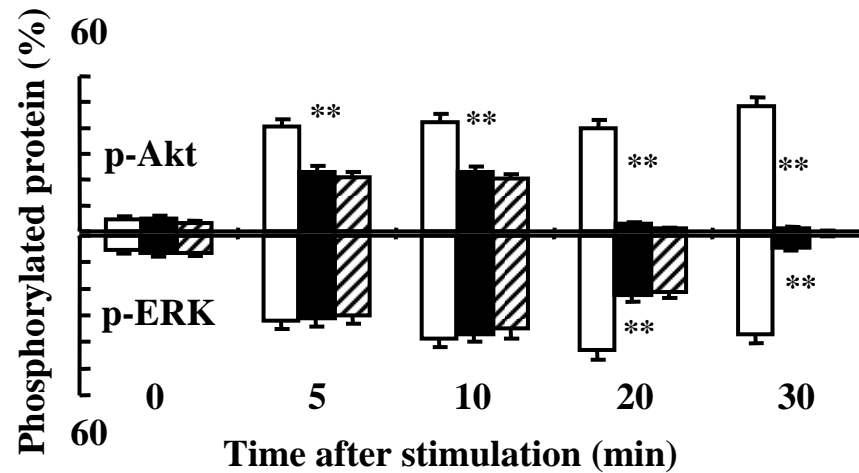
Supplemental Fig. 1. C5aR agonist-induced effect of C5a/RP S19 on guinea pig cutaneous mast cells. (A), In comparison with C5a (white circles), the plasma-extravasation activity of C5a/RPS19 (black circles) was measured in guinea pig skin. The absorbance of extravasated Evans blue dye was measured at 620 nm. Results were expressed as a mean amount of extravasated dye/lesion  $\pm$  SD (n=4). (B), In the competitive experiment, C5a was injected in the simultaneous presence of C5a/RP S19. Data is expressed as the percent ratio to the C5a-induced plasma extravasations (n=4). P values between C5a with and without C5a/RPS19 of less than 0.05 were considered to indicate statistical significance ( $P < 0.05$ : \*,  $P < 0.01$ : \*\*).

## Supplemental Figure 2



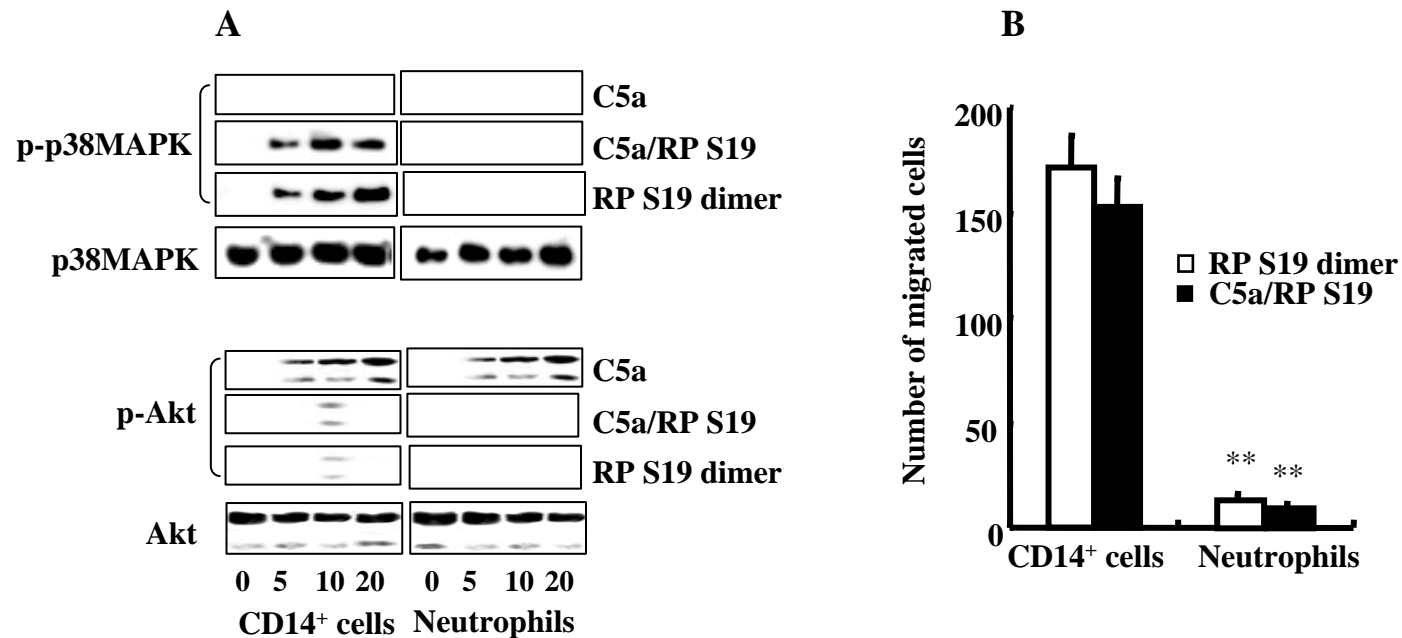
Supplemental Fig. 2. C5aR agonist-induced effect of C5a/RP S19 on guinea pig abdomen mast cells. (A), In addition to C5a (white circles), an agonistic effect of C5a/RP S19 (black circles) was observed in chemotaxis assays. (B), In the competitive experiment, resident mast cells were stimulated with C5a in the simultaneous presence (black columns) or absence (white columns) of various concentrations of C5a/RP S19. Results were expressed the number of migrated cells. Data is expressed as mean  $\pm$  SD (n=4). P values of less than 0.05 between C5a with and without C5a/RPS19 were considered to indicate statistical significance ( $P < 0.05$ : \*,  $P < 0.01$ : \*\*)

### Supplemental Figure 3



Supplemental Fig. 3. HMC-1 cells were collected at various time points after stimulation with C5a (white columns), C5a/RP S19 (black columns), or a mixture (hatched columns) (see Fig. 3B). Akt and ERK phosphorylation were detected by western blot. Data is expressed as mean  $\pm$  SD (n=4). P values less than 0.05 were considered to indicate statistical significance (P<0.01: \*\*).

## Supplemental Figure 4



Supplemental Fig. 4. (A), Human CD14<sup>+</sup> cells ( $2 \times 10^6$  cells/ml) and neutrophils ( $2 \times 10^6$  cells/ml) were collected at various time points after a stimulation with  $10^{-8}$  M C5a,  $10^{-7}$  M C5a/RP S19, and  $10^{-8}$  M RP S19 dimer, respectively. Akt and p38MAPK phosphorylations were detected by western blotting. (B), In comparison with  $10^{-8}$  M RP S19 dimer (white columns), an agonistic and an antagonistic effects of  $10^{-7}$  M C5a/RP S19 (black columns) were observed in chemotaxis assay. Data is expressed as mean  $\pm$  SD (n=4). P values of less than 0.05 between C5a with and without C5a/RPS19 were considered to indicate statistical significance ( $P < 0.01$ : \*\*)

**Figure 1**

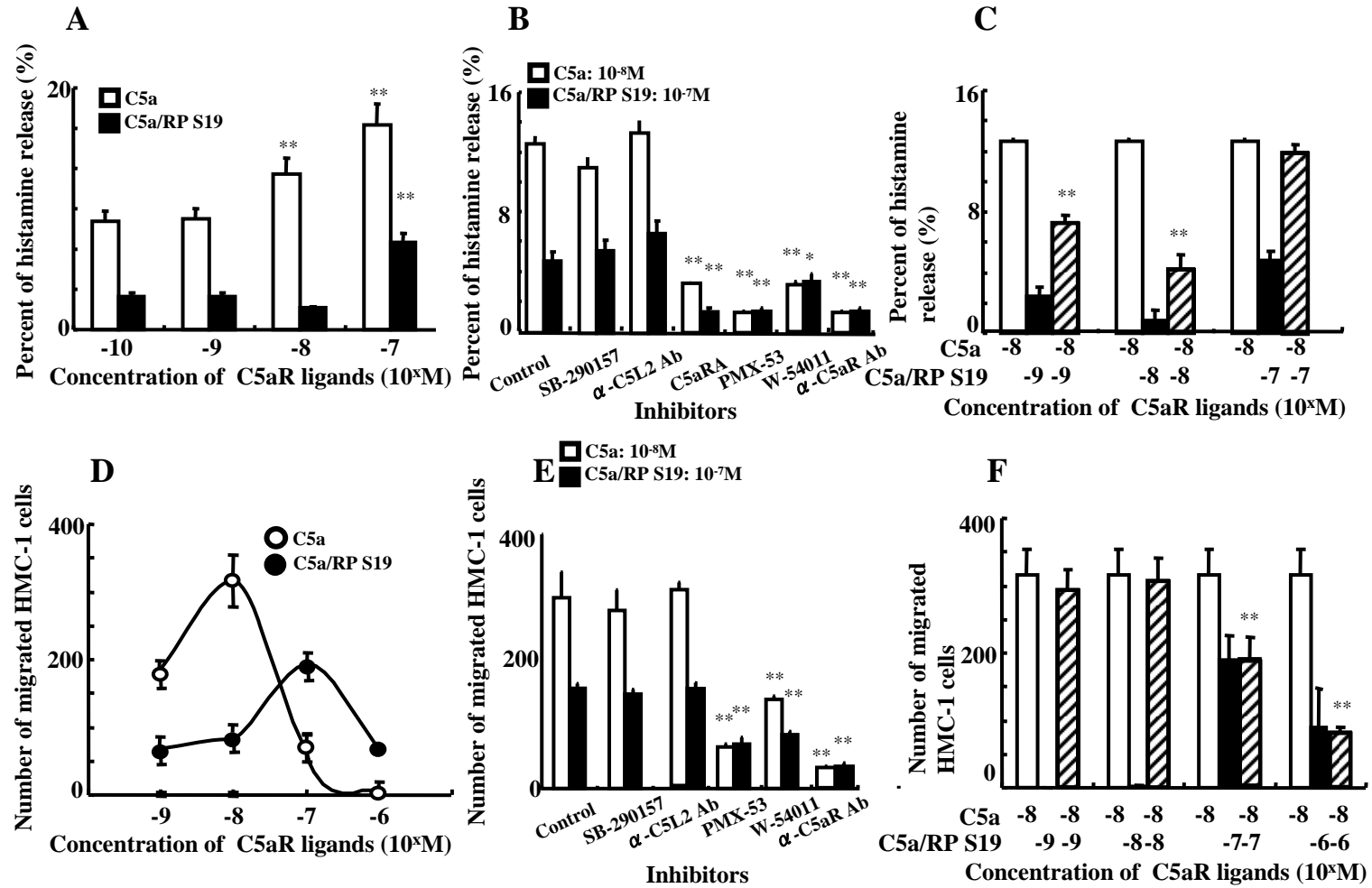


**Figure 2**

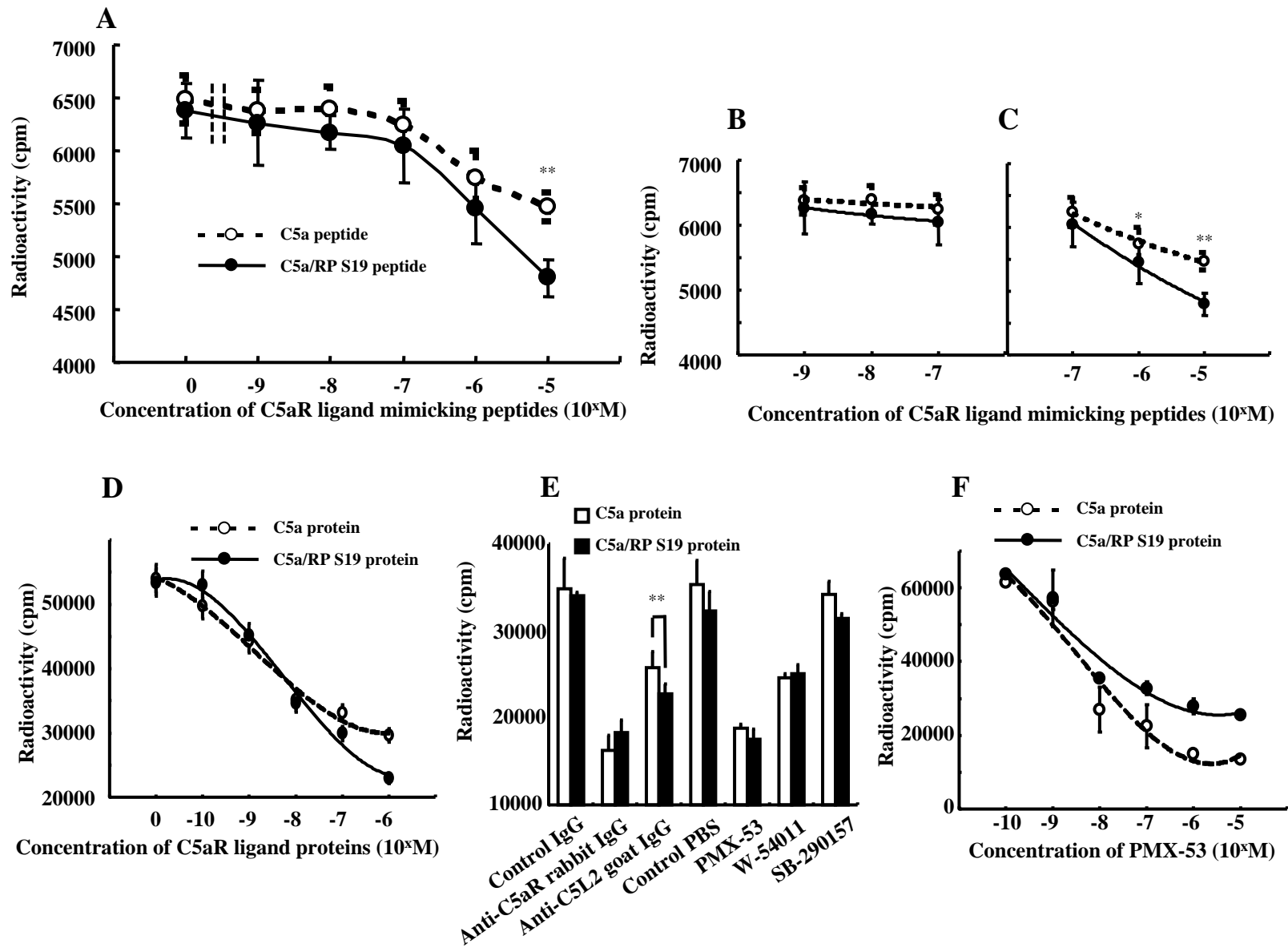


**Figure 3**

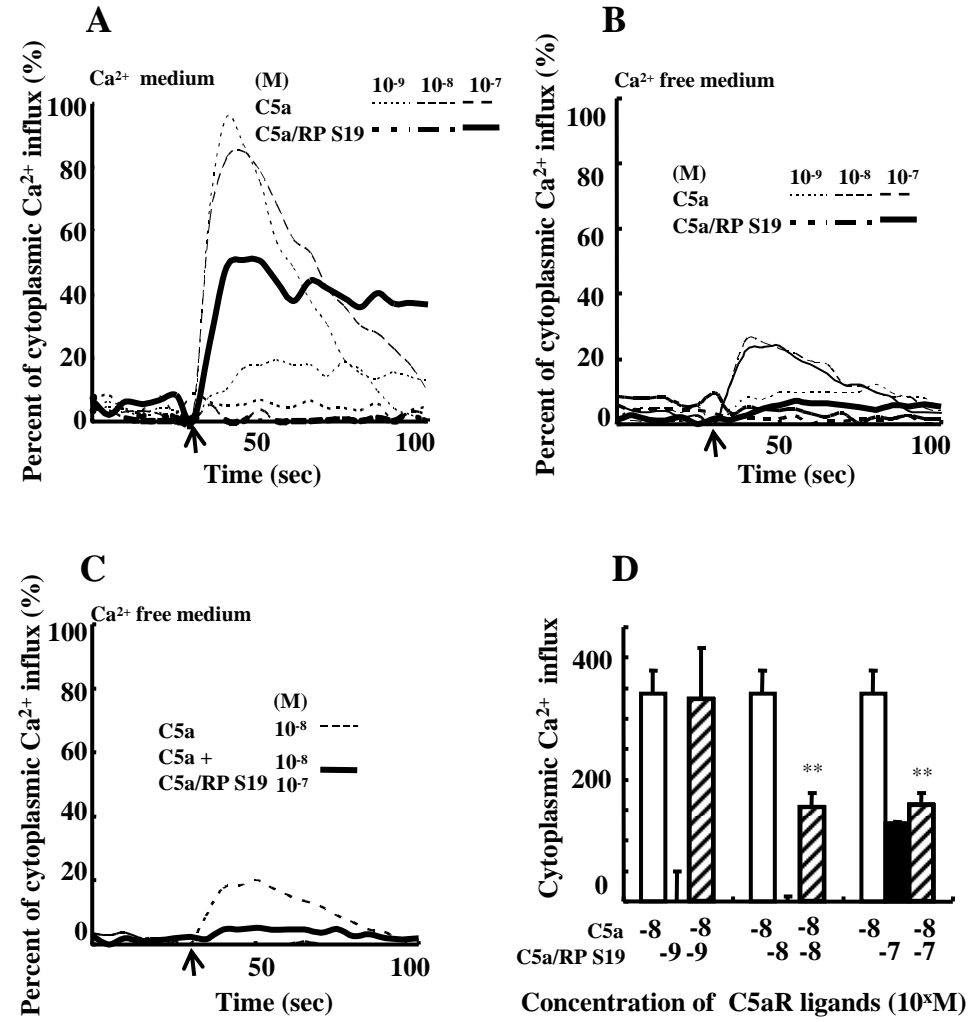
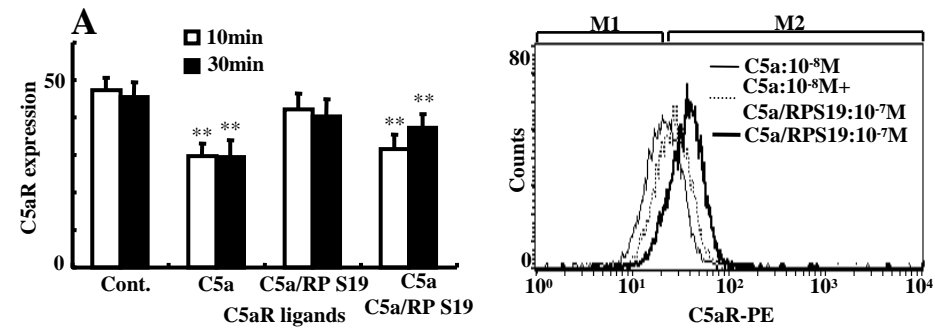


**Figure 4**



**B**



**C**

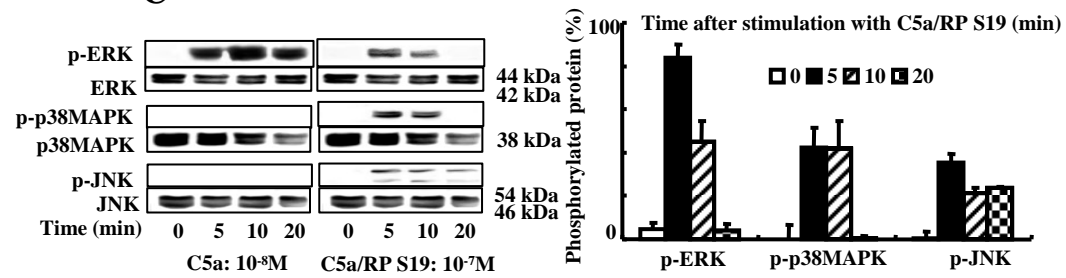


**Figure 5**

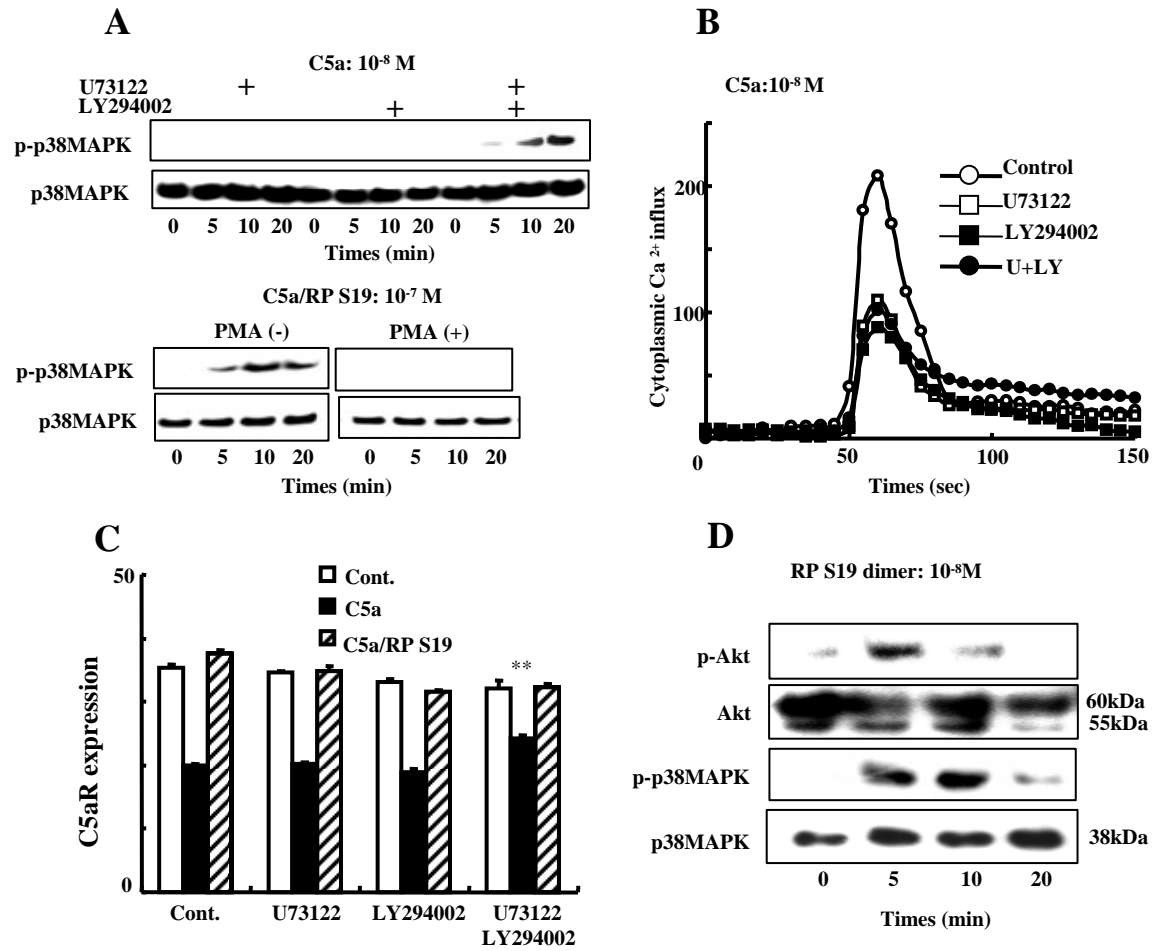


**Figure 6**

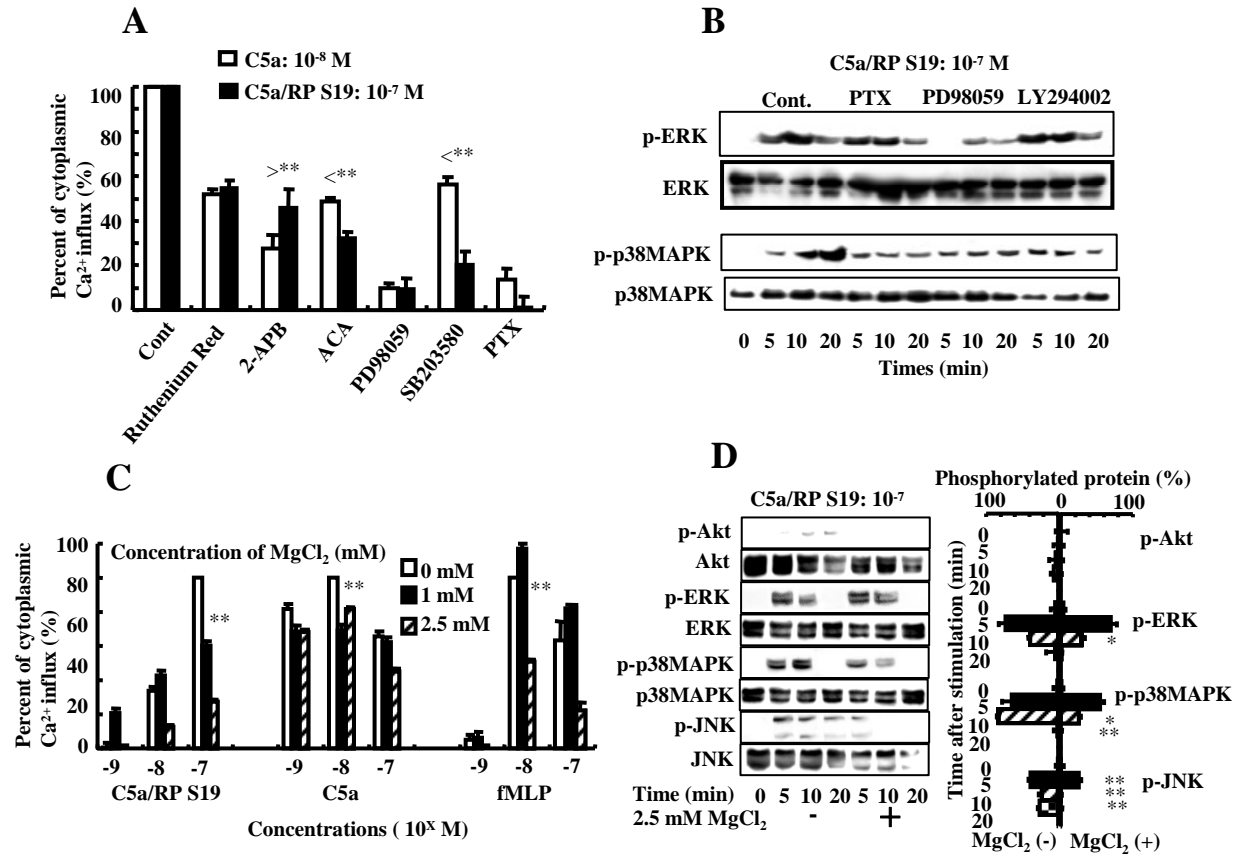


**Figure 7**

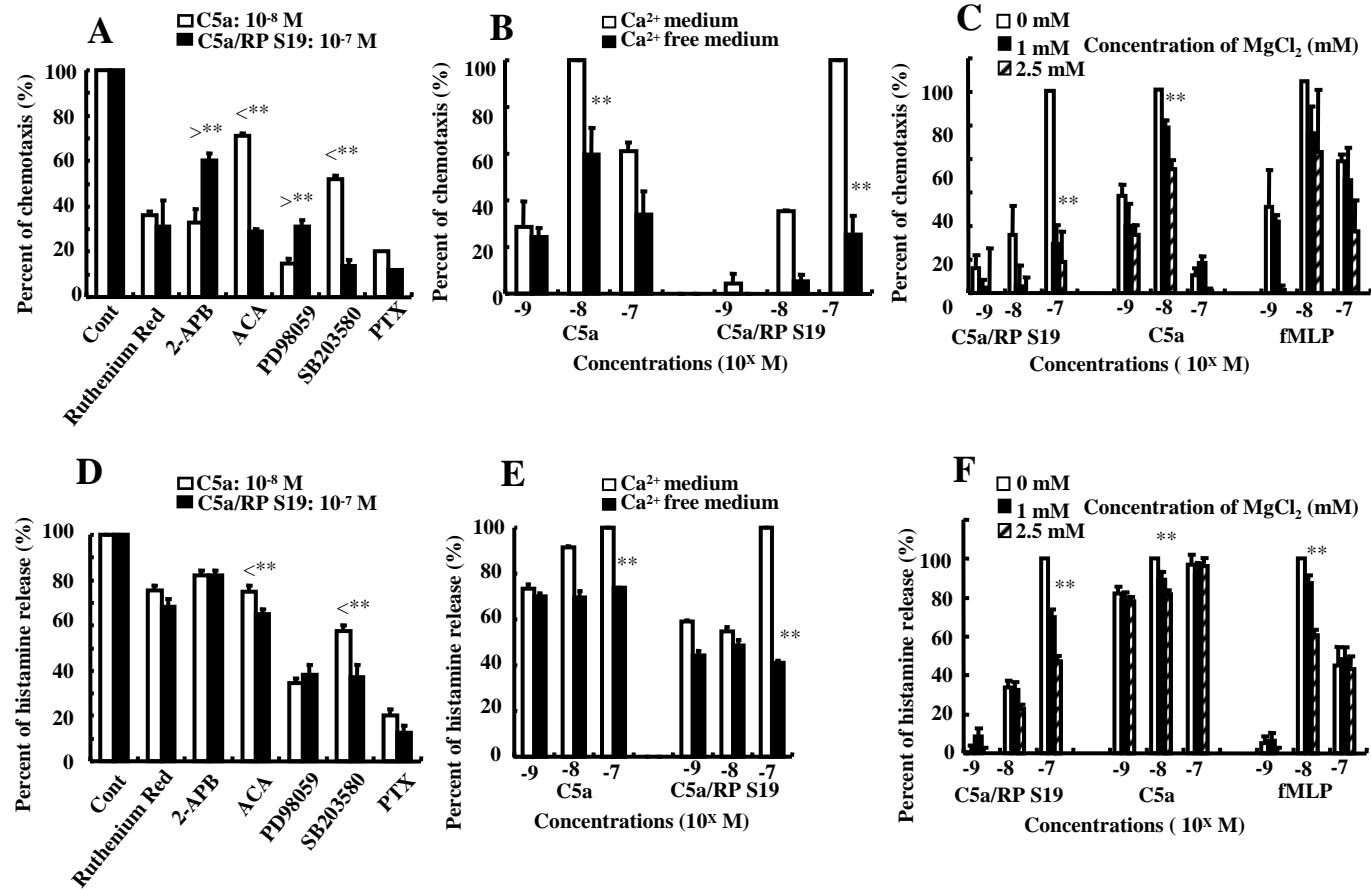


**Figure 8**

